



Bundesministerium
für Bildung
und Forschung

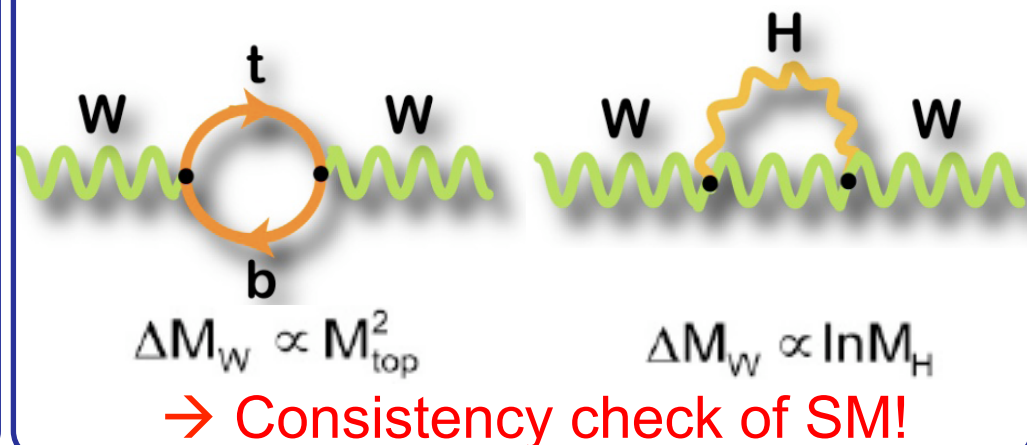




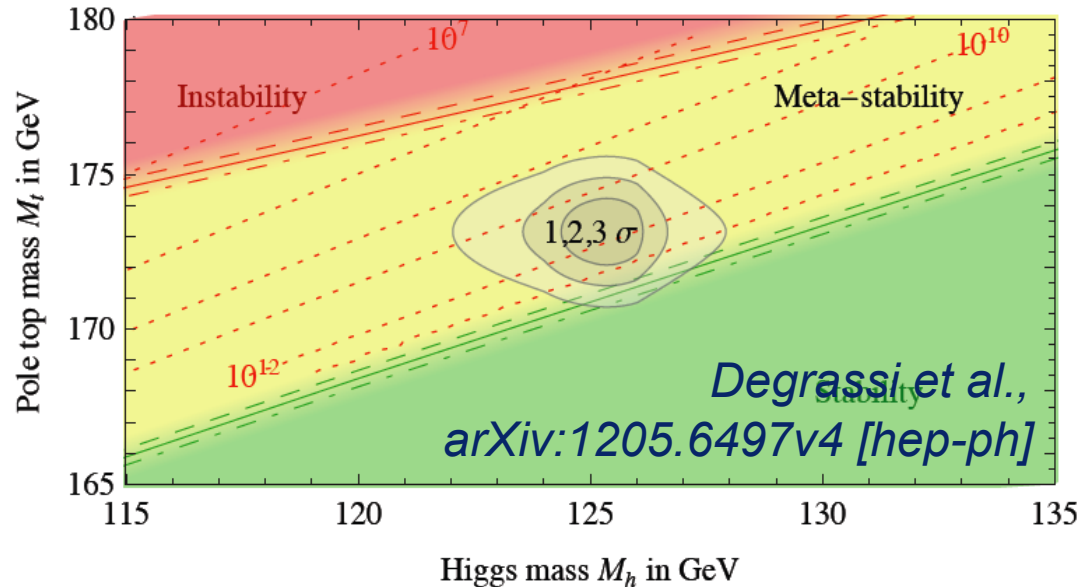
The top quark is special:
it is the **heaviest SM quark!**

- Why is it so heavy?
- Does it play a special role in EW symmetry breaking?

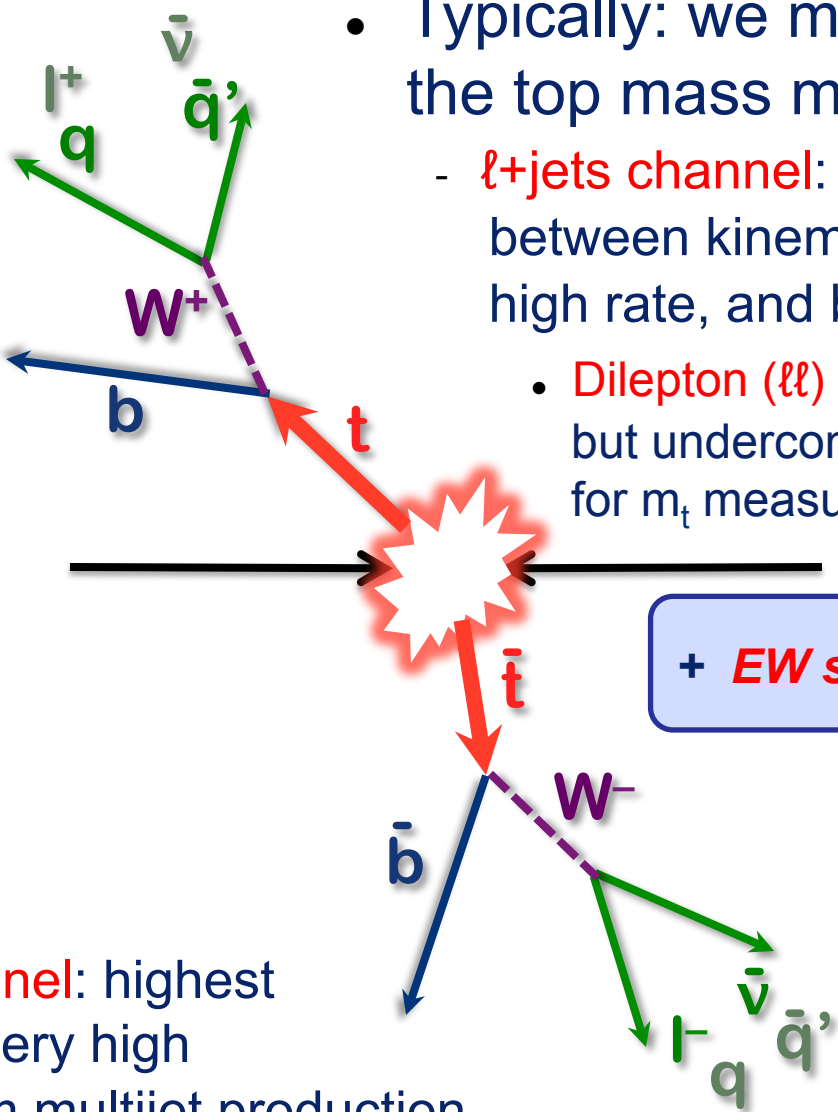
Overconstrain M_{Higgs} , m_t , and M_W :



The uncertainty on the top quark mass has the biggest impact on the stability of the Universe from the positiveness of the Higgs quartic self-coupling:



Definition of decay channels

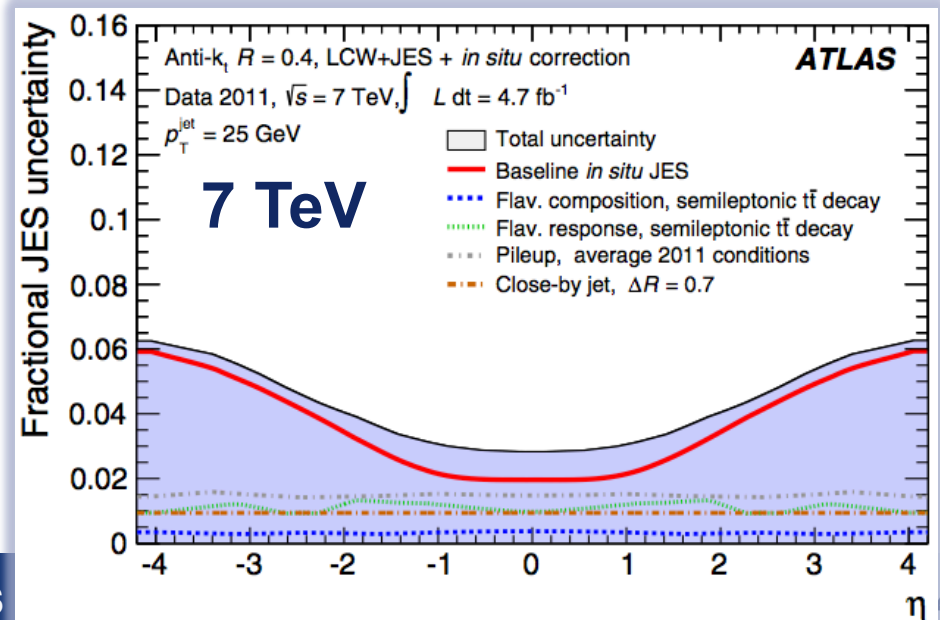
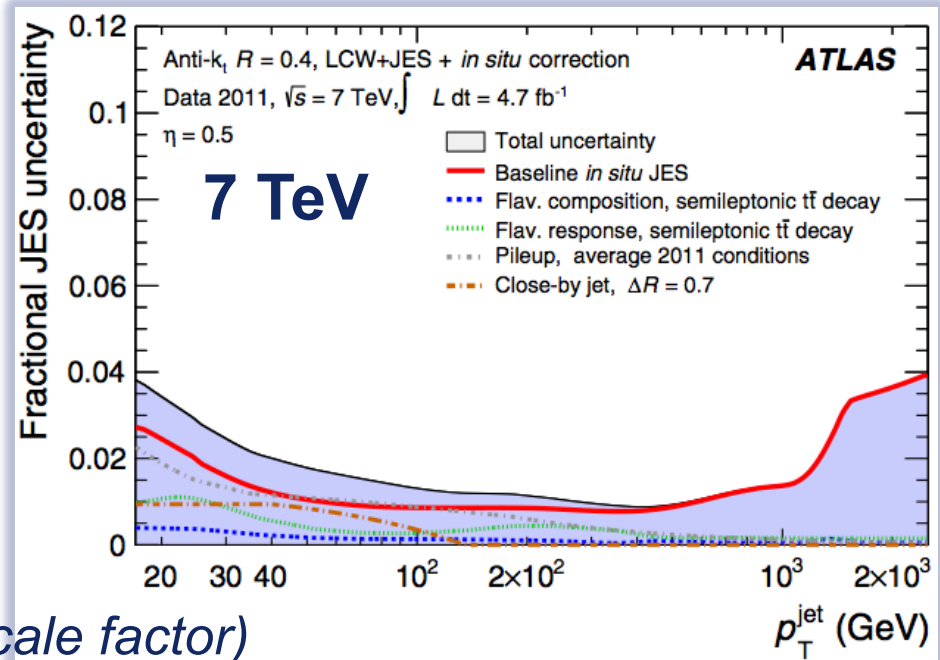
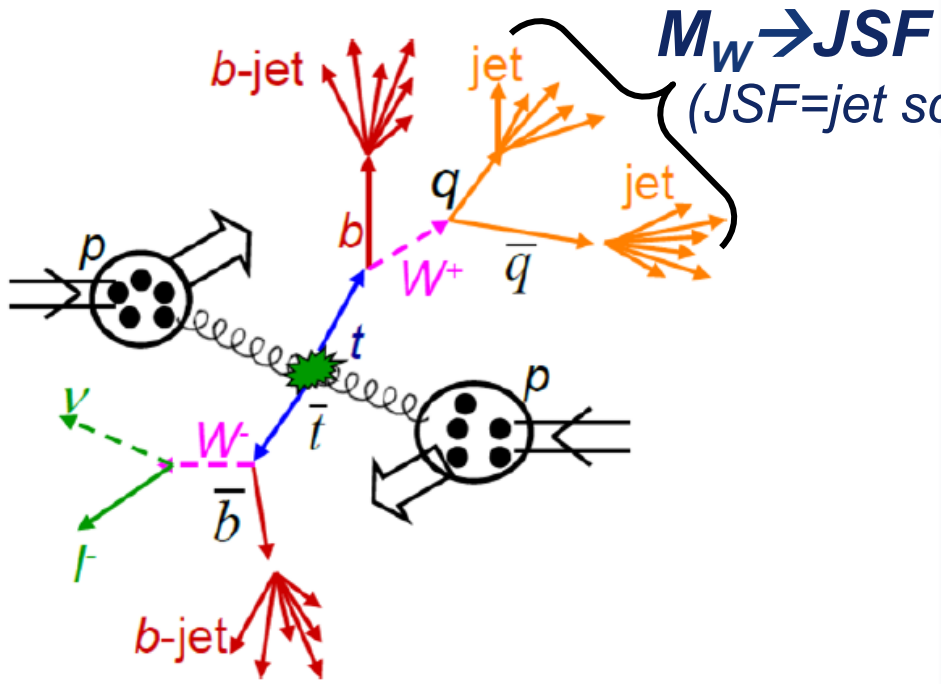


- Typically: we measure the top mass m_t in $t\bar{t}$ events:
 - **$l+jet$ channel:** good compromise between kinematic reconstruction, high rate, and backgrounds
 - **Dilepton (ll) channel:** low backgrounds, but underconstrained kinematics for m_t measurement and low rate
 - **All-hadronic channel:** highest branching ratio, very high backgrounds from multijet production

+ ***EW single top production***

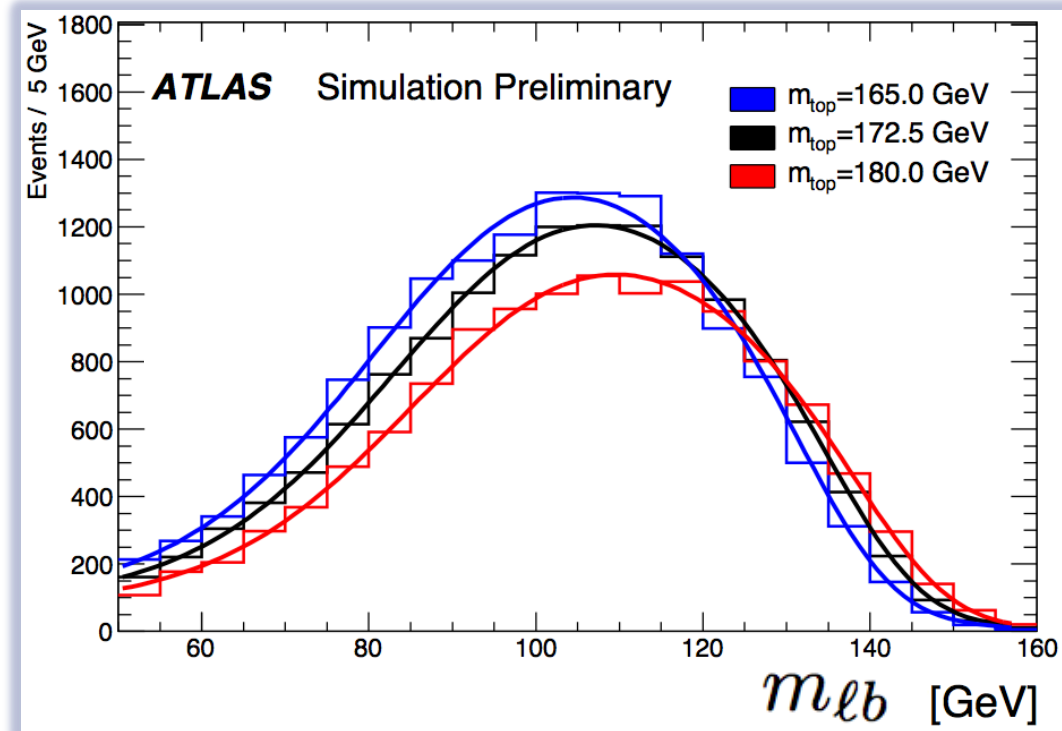


- Sizeable uncertainty from jet energy scale (JES):
 - $\approx 1.5\%$ for central $|\eta|$, intermediate p_T ,
 - up to $\approx 5\%$ else
- Calibrate JES in-situ:





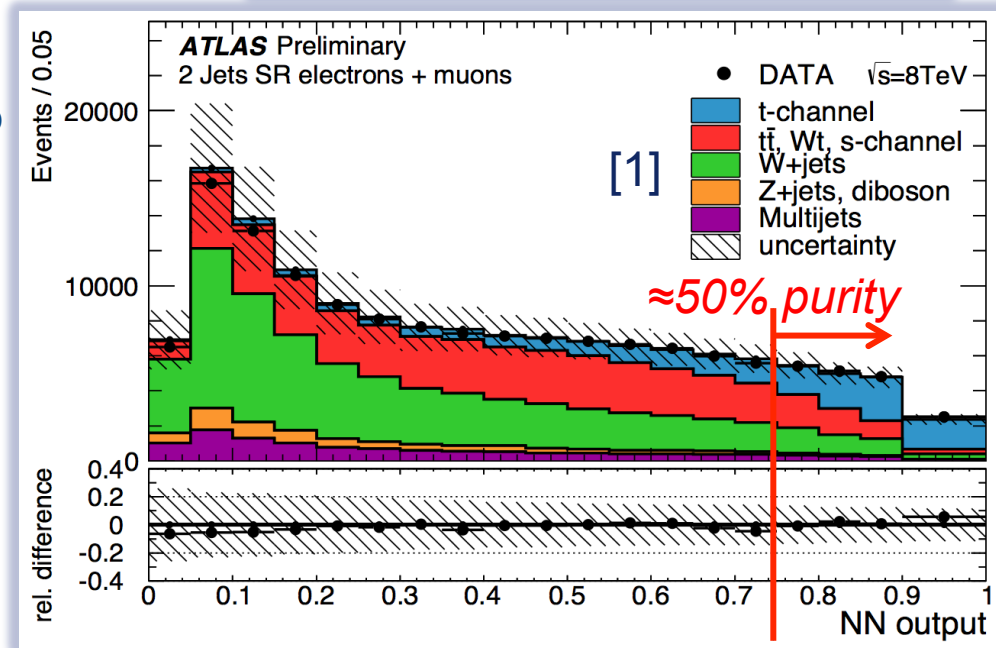
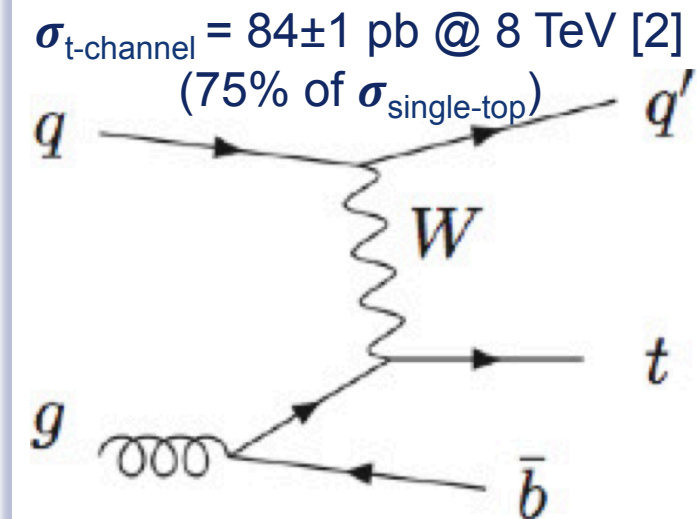
- World's first measurement of m_t in topologies enriched with single top events ($\sqrt{s}=8$ TeV, 20.3 fb^{-1}) [1]
- Apply template method using the observable $m_{\ell b}$:
 - Invariant mass of $\ell+b$ system
 - → reduced sensitivity to systematic uncertainties
- Signal templates:
 - Use simulated single top and tT events
 - Parametrised in m_t
- Background template:
 - All other processes



[1] ATLAS-CONF-2014-055 (2014)



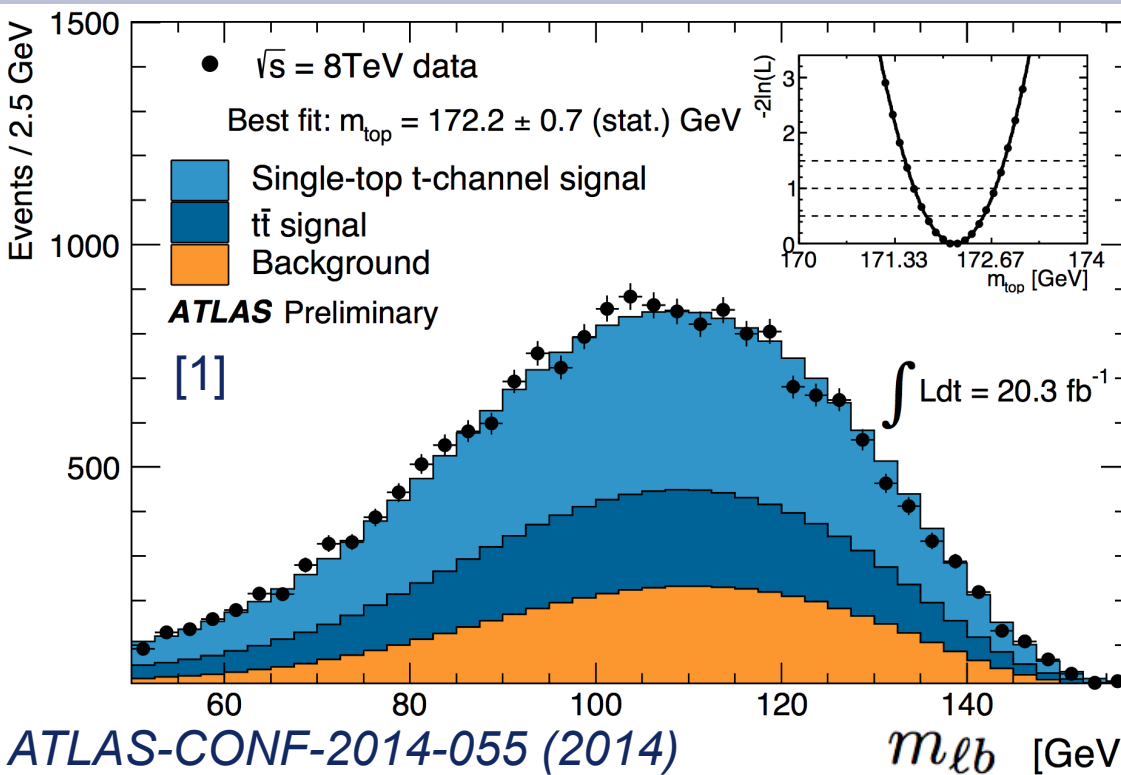
- Focus on ***t*-channel** process
 - High cross section
 - Best S/B for single top at LHC
- Preselection:
 - 1 high- p_T ℓ , high E_T^{miss}
 - ≥ 2 High- p_T jets $|\eta| < 3.5$, 1 b-tag
- Construct **neural network**:
 - 12 variables like $m_{\ell vb}$ and m_{jb}
- Extract m_t in **NN>0.75**
- Orthogonal control region:
 - Constrain $W + \text{jets}$



[1] ATLAS-CONF-2014-055 (2014)

[2] PLB 736, 58 (2014)

m_t in single top events (III)



Dominant systematics:

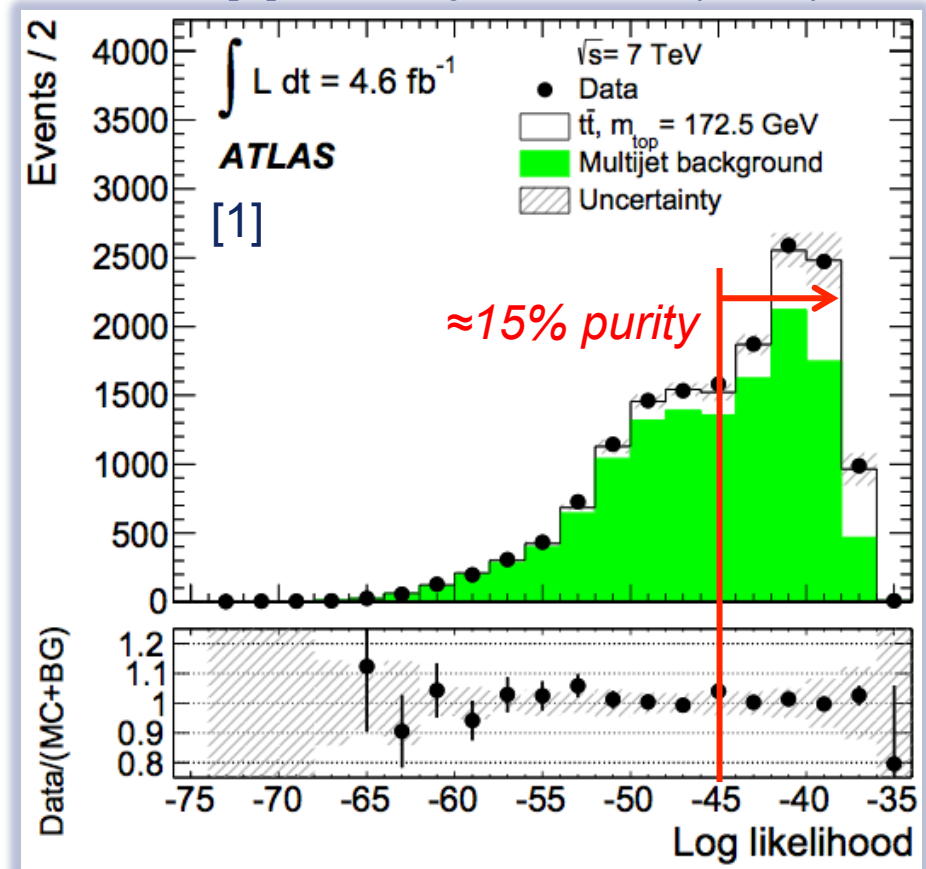
- JES (1.5 GeV):
 - large uncertainty in $2.75 < |\eta| < 3.5$
- Hadronisation (0.7 GeV)
 - Change in spectra from matching of ME to parton shower
- W+jets bgr. (0.4 GeV)
 - Similar shape in m_{lb}

$$m_t = 172.2 \pm 0.7 \text{ (stat)} \pm 2.0 \text{ (syst)} \text{ GeV},$$

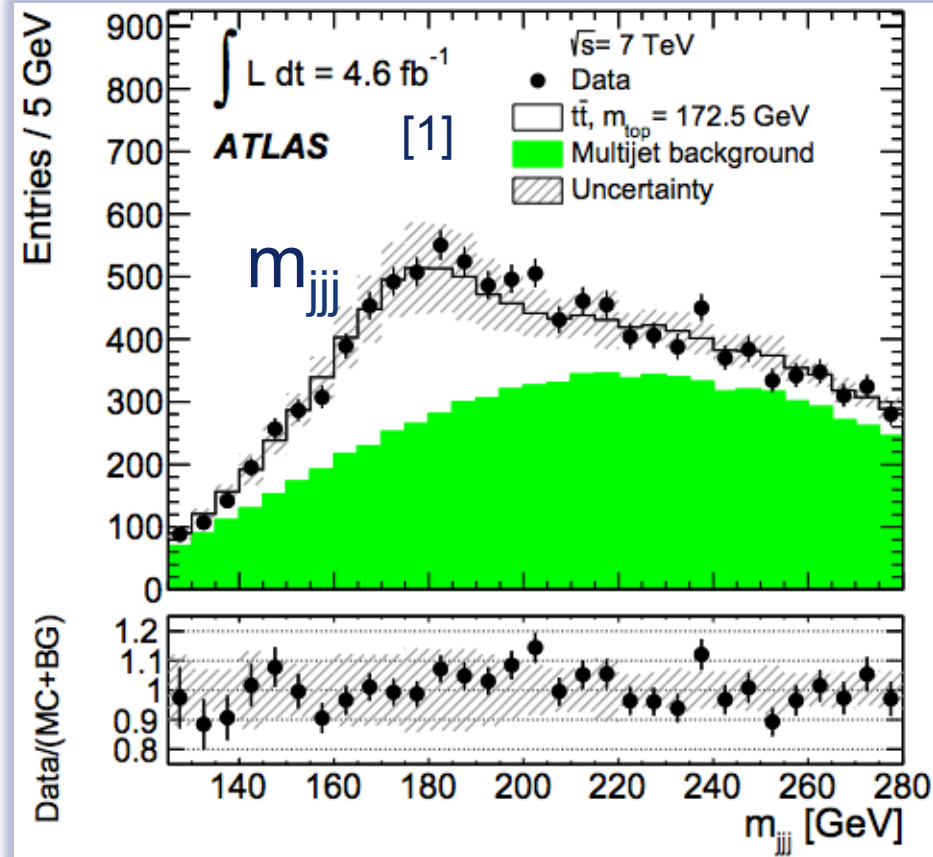
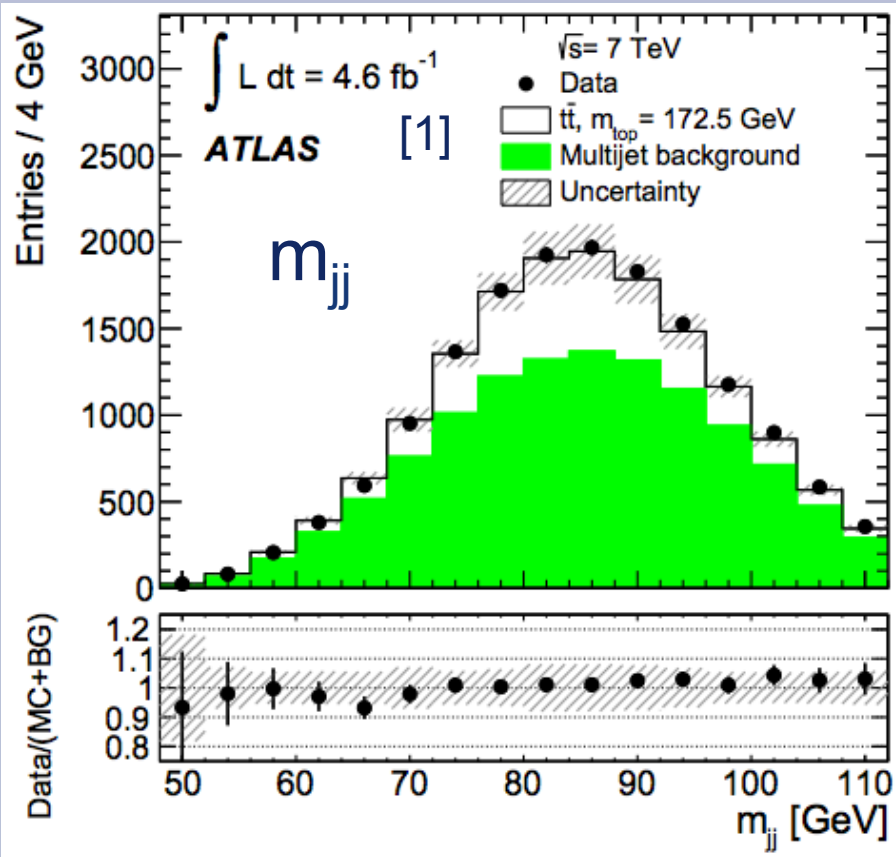
- Complementary contribution to world average:
 - Lower Q^2 -regime compared to tT
 - Different backgrounds, different colour connections

- Template method using $R_{3/2} = m_{jjj}/m_{jj}$ ($\sqrt{s}=7 \text{ TeV}, 4.6 \text{ fb}^{-1}$) [1]
 - m_{jj} : jets matched to $W \rightarrow q' \bar{q}$
 - m_{jjj} : jets matched to $t \rightarrow q' \bar{q} b$
 → reduced sensitivity to Δ_{JES}
- Selection:
 - no high- p_T ℓ , no E_T^{miss}
 - ≥ 5 jets with $p_T > 55 \text{ GeV}$
 - 6th jet with $p_T > 30 \text{ GeV}$
 - 2 b-tags
 - + topological selections
- Reconstruct tT system using kinematic likelihood fit
 - Assign jets to partons
 - Enhance purity

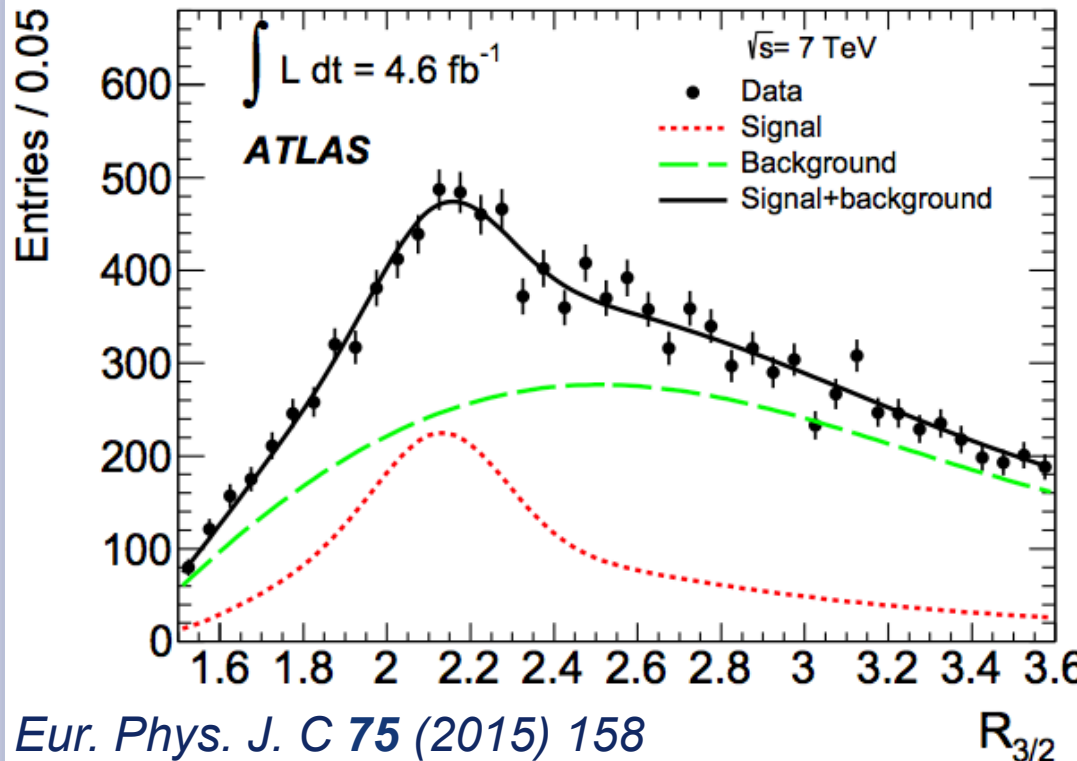
[1] Eur. Phys. J. C 75 (2015) 158



- Model MJ background (shape+norm) using control regions in:
 - 6th jet p_T
 - b-tag multiplicity



[1] Eur. Phys. J. C 75 (2015) 158



$$m_t = 175.1 \pm 1.4 \text{ (stat.)} \pm 1.2 \text{ (syst.) GeV}$$

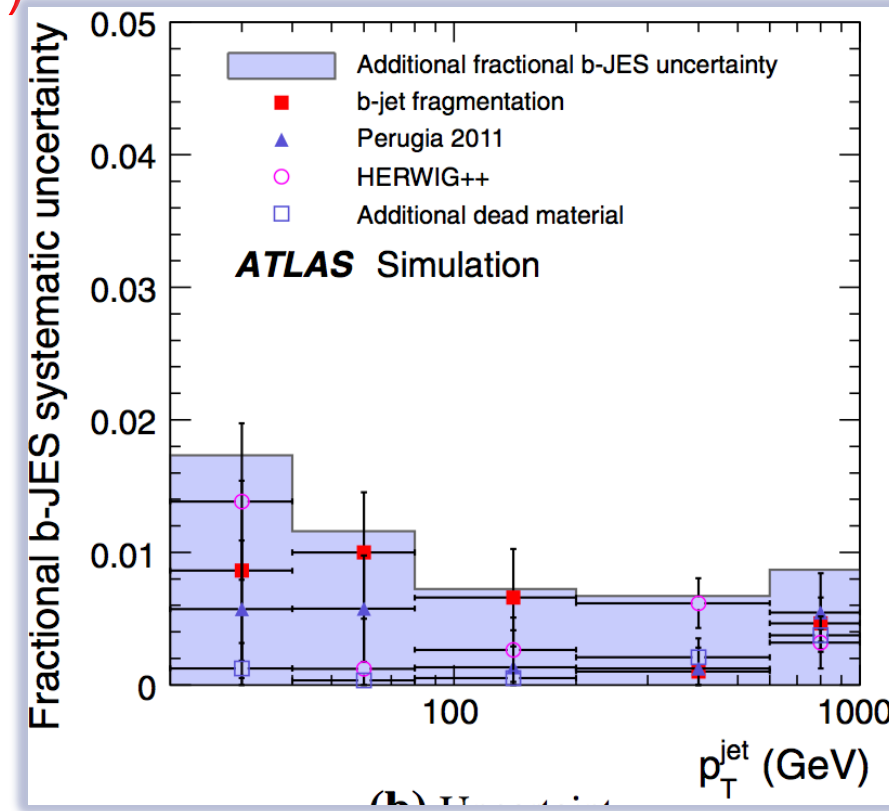
Dominant systematics:

- JES (0.5 GeV)
 - Detector description
- b-quark JES (0.6 GeV)
 - difference: b-quark jets and jets from $W \rightarrow q' \bar{q}$
- Hadronisation (0.5 GeV)
 - Same as single top
- MJ modelling (0.4 GeV)
 - Sideband choice

- Valuable contribution to world average:

- Relative precision $\approx 1\%$
 - Different backgrounds, mostly data-driven

- Typical largest uncertainties for m_t :
 - b-quark JES versus overall JES
- ATLAS: m_t in $\ell + \text{jets}$, $\sqrt{s}=7 \text{ TeV}$, 4.6 fb^{-1} [1]
 - In-situ calibration of overall JES (JSF)
 - In-situ calibration of b-JES (bJSF)
 - Relative to JES for u,d,c,s,g
- Selection:
 - 1 high- p_T ℓ , high E_T^{miss}
 - ≥ 4 High- p_T jets, ≥ 1 b-tag
- Reconstruction of tT system through kinematic likelihood fit
 - Similar to all-hadronic result

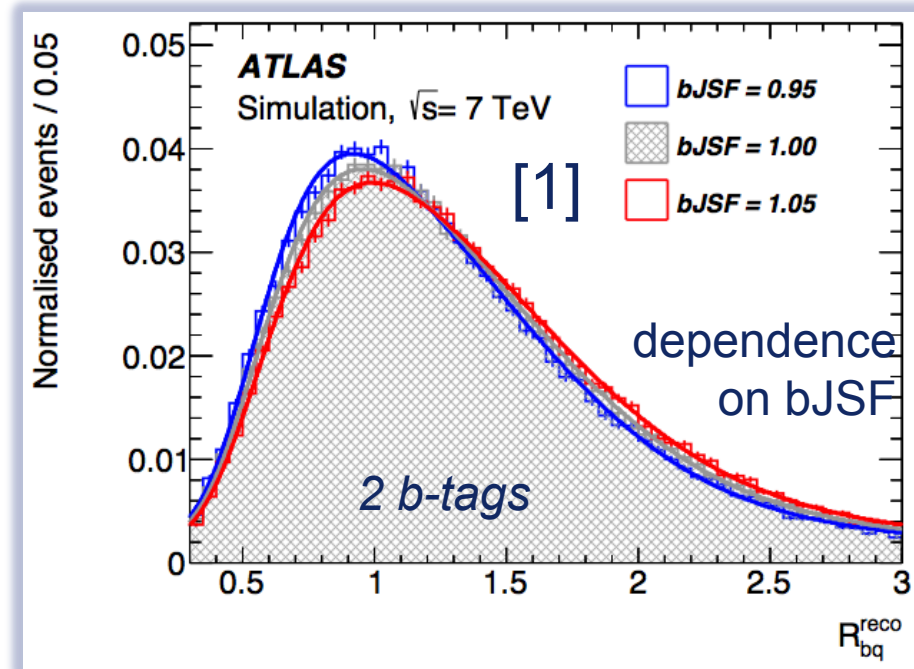
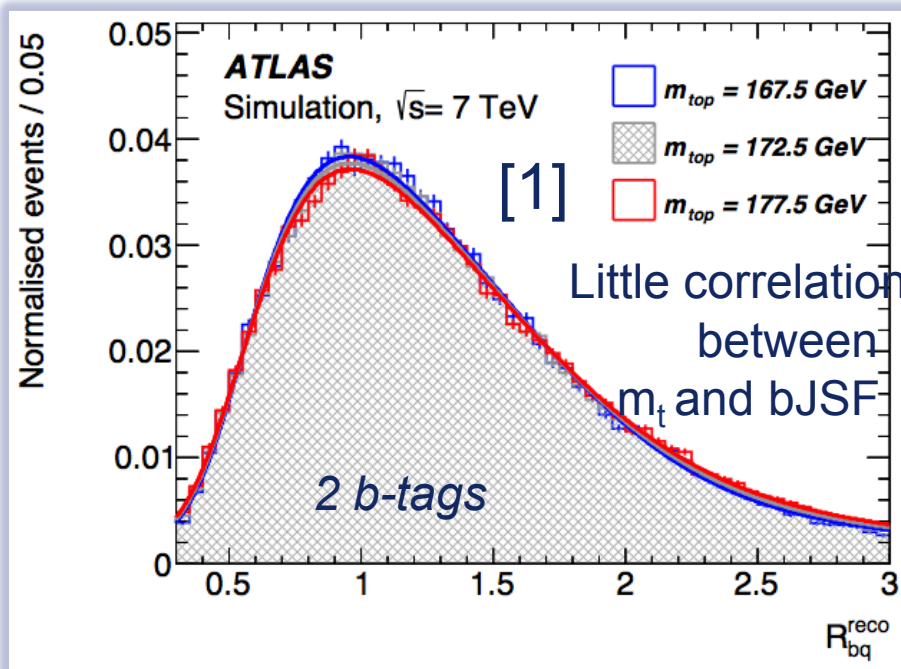


[1] subm. to EPJC, arXiv:1503.05427

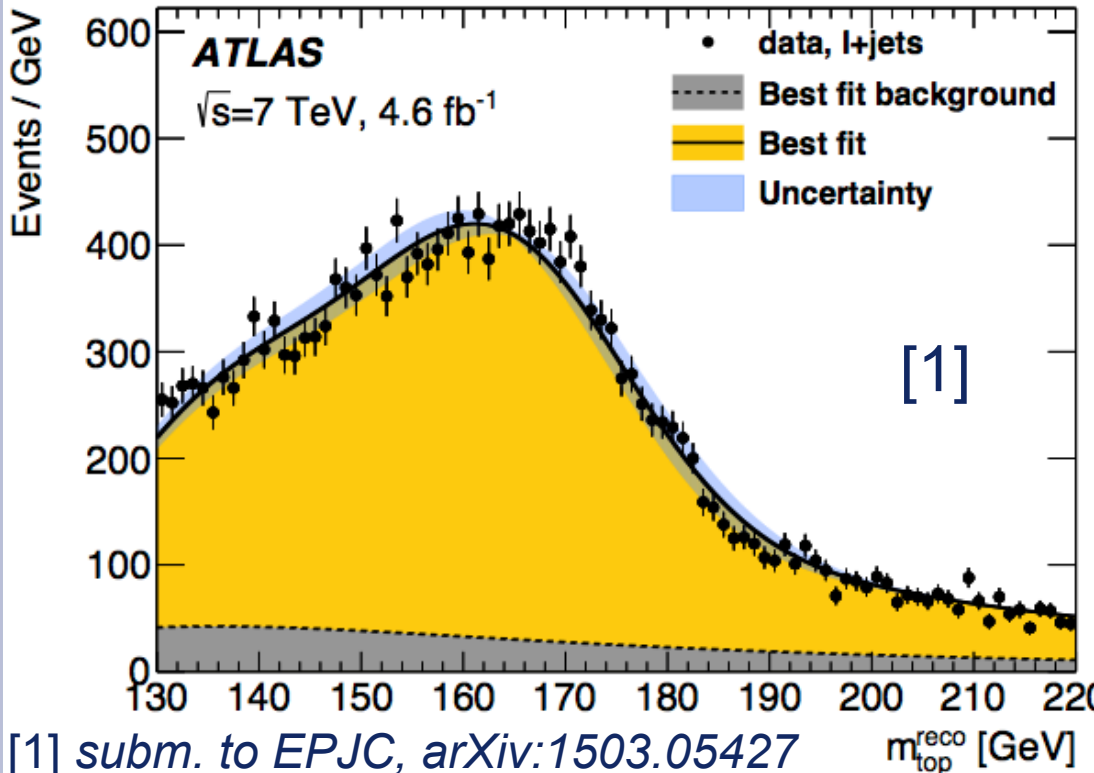
- Introduce R_{bq} variable to provide sensitivity to bJSF:

$$R_{bq}^{\text{reco},2\text{b}} = \frac{p_T^{b_{\text{had}}} + p_T^{b_{\text{lep}}}}{p_T^{W_{\text{jet}_1}} + p_T^{W_{\text{jet}_2}}}$$

$$R_{bq}^{\text{reco},1\text{b}} = \frac{p_T^{b_{\text{tag}}}}{(p_T^{W_{\text{jet}_1}} + p_T^{W_{\text{jet}_2}})/2}$$



[1] subm. to EPJC, arXiv:1503.05427



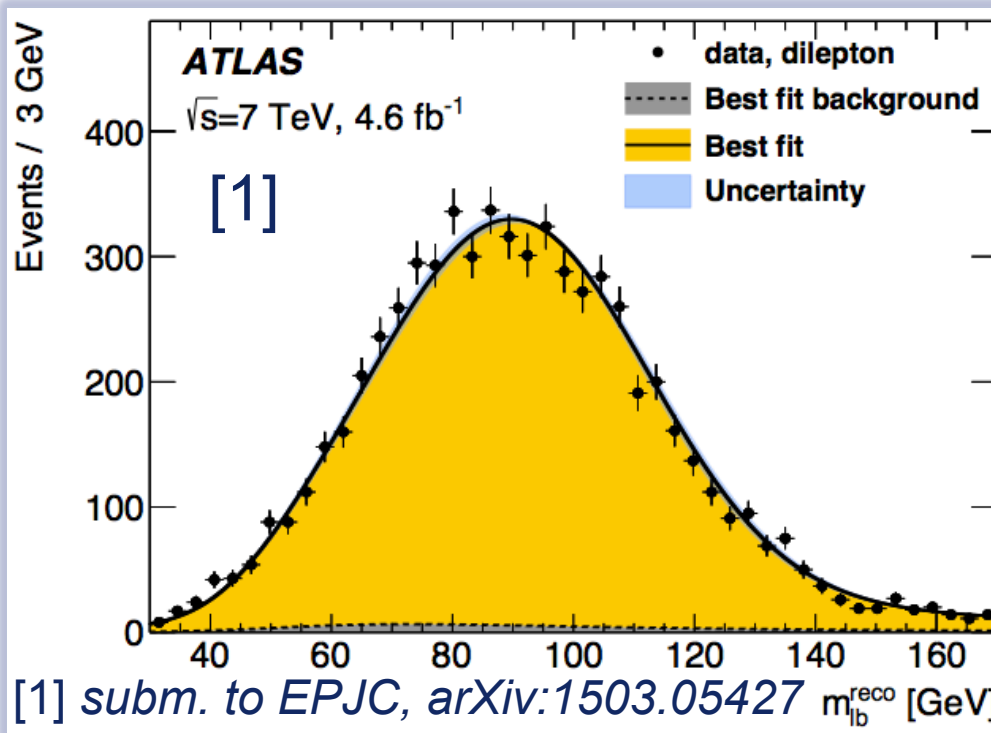
Dominant systematics:

- JES (0.58 GeV)
 - Detector description
- b-quark JES (0.06 GeV)
 - Eliminated → statistical
- b-tagging (0.50 GeV)
 - b-tagging uncertainty as function of p_T changes R_{bq} shape

$$m_{\text{top}}^{\ell+\text{jets}} = 172.33 \pm 0.75 \text{ (stat + JSF + bJSF)} \pm 1.02 \text{ (syst) GeV,}$$

- ATLAS' strongest contribution to world average:
 - Relative precision $\approx 0.7\%$
 - Statistical limitations, expect improved precision for 8 TeV

- Utilise clean dilepton channel at $\sqrt{s}=7$ TeV, 4.6 fb^{-1} [1]
 - Apply template method using the observable $m_{\ell b}$:
 - Same as in single-top result, reduced sensitivity to syst. uncert.
 - Selection similar to $\ell+\text{jets}$ but with 2 leptons and ≥ 2 jets



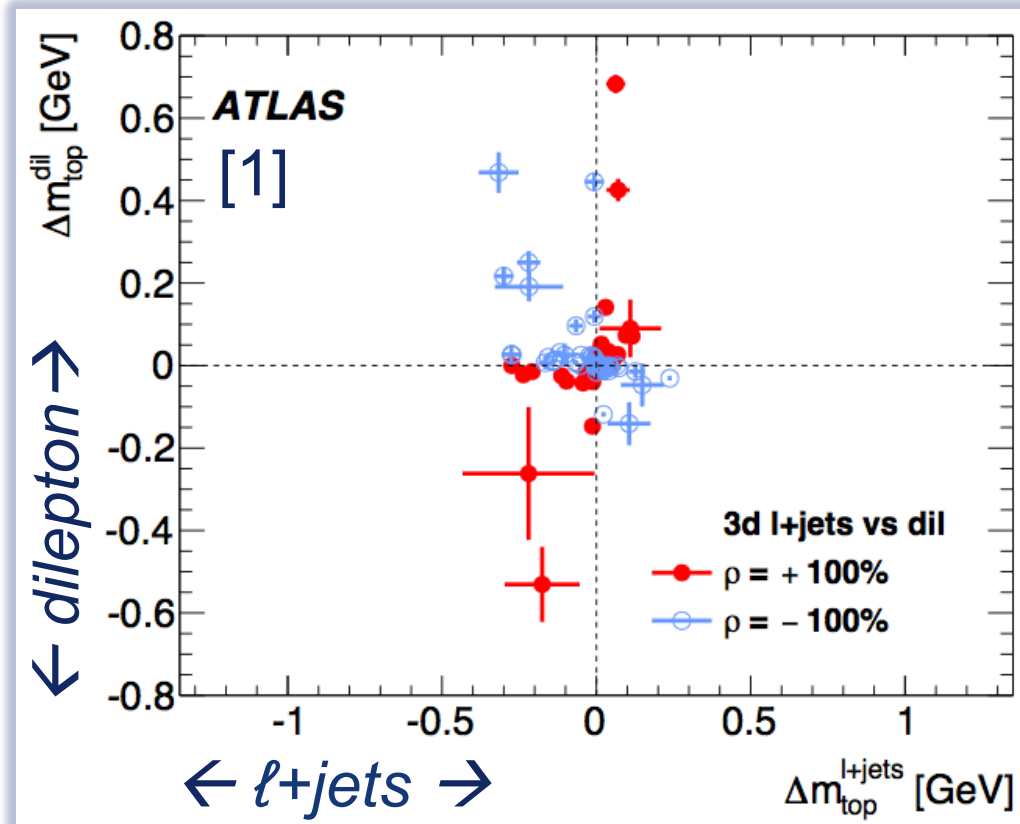
Dominant systematics:

- JES (0.75 GeV)
 - Detector description
- b-quark JES (0.68 GeV)
 - Detector description
- Hadronisation (0.53 GeV)
 - changes $m_{\ell b}$ shape
- ISR/FSR (0.47 GeV)
 - jet-parton assignments

$$m_{\text{top}}^{\text{dil}} = 173.79 \pm 0.54 \text{ (stat)} \pm 1.30 \text{ (syst)} \text{ GeV.} \quad \approx 0.9\%$$



- Combine ℓ +jets and dilepton results [1] with BLUE
- Correlations ρ in the effect of systematic uncertainties Δm_t between ℓ +jets and dilepton:
 - ρ signs are statistically significant for all large systematics!
- Substantial gains in combination:
 - $\approx 0.5\%$ precision!



$$m_{\text{top}}^{\text{comb}} = 172.99 \pm 0.48 \text{ (stat)} \pm 0.78 \text{ (syst)} \text{ GeV} = 172.99 \pm 0.91 \text{ GeV.}$$



Alternative measurements

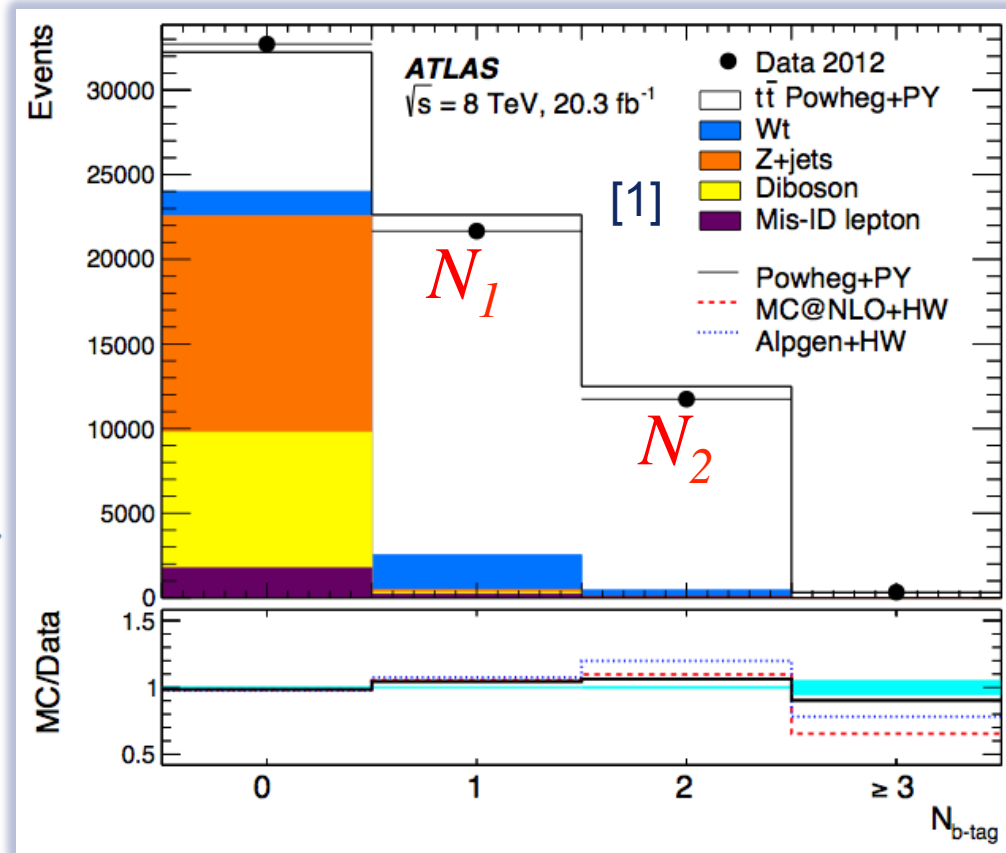
[1] EPJC 74, 3109 (2014), [2] PRL 110, 252004 (2013)

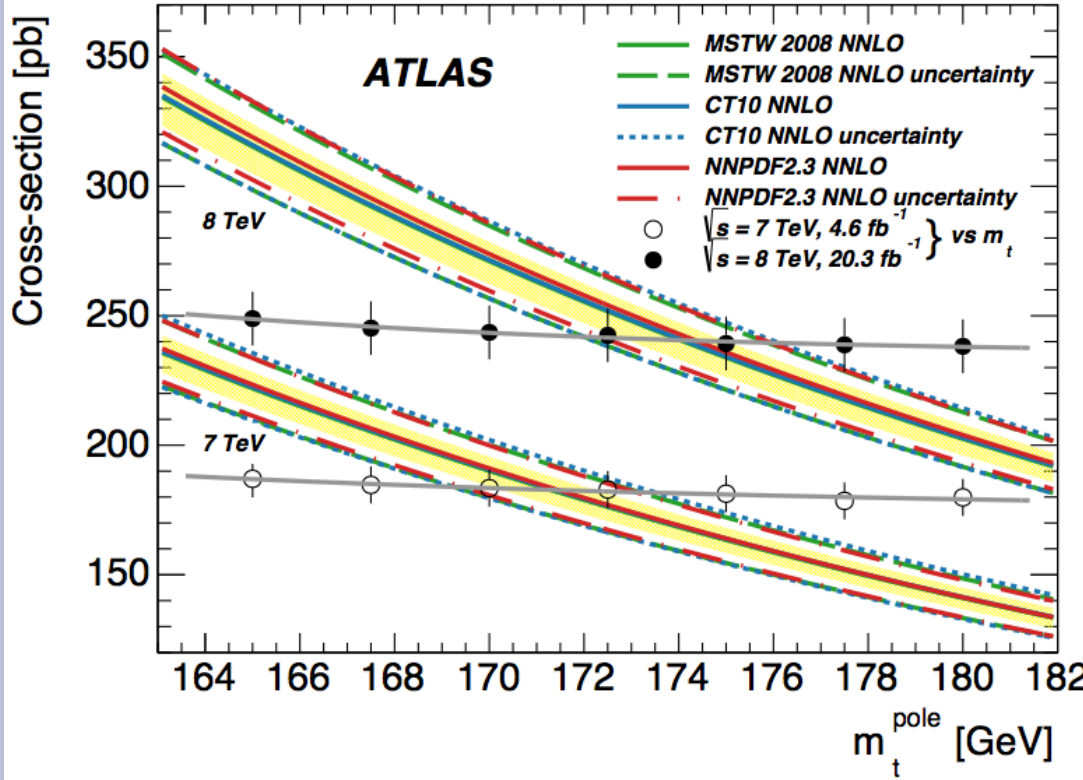
- Experiment:
 - World's most precise measurement of m_t from $\sigma_{t\bar{t}}$ [1], $\Delta\sigma_{t\bar{t}}: \approx 4\%$!
- Theory:
 - Recent NNLO+NNLL calculation [2], $\Delta\sigma_{t\bar{t}}: \approx 3\%$!
- Selection:
 - Similar to dilepton m_t
 - $e^\pm \mu^\mp$, no topological cuts
- Fit b-tagging efficiency \times acceptance \times reco eff. ε_b together with $\sigma_{t\bar{t}}$:

$$N_1 = \int dt \mathcal{L} \times \sigma_{t\bar{t}} \varepsilon_{e\mu} \times 2\varepsilon_b (1 - C_b \varepsilon_b) + N_1^{\text{bgr}}$$

$$N_2 = \int dt \mathcal{L} \times \sigma_{t\bar{t}} \varepsilon_{e\mu} \times C_b \varepsilon_b^2 + N_2^{\text{bgr}},$$

- Minimal use of MC simulations $C_b = \varepsilon_{bb}/\varepsilon_b$





$$\begin{aligned} m_t^{\text{pole}} &= 171.4 \pm 2.6 \text{ GeV } (\sqrt{s} = 7 \text{ TeV}) \\ m_t^{\text{pole}} &= 174.1 \pm 2.6 \text{ GeV } (\sqrt{s} = 8 \text{ TeV}). \end{aligned}$$

- World's most precise m_t^{pole} from σ_{tT}
 - Precision in the same ballpark as direct methods: $\approx 1.5\%$!

- Hard gluon radiation off top quark $\sigma_{t\bar{t}+1\text{-jet}}$ depends on m_t :

$$\mathcal{R}(m_t^{\text{pole}}, \rho_s) = \frac{1}{\sigma_{t\bar{t}+1\text{-jet}}} \frac{d\sigma_{t\bar{t}+1\text{-jet}}}{d\rho_s}(m_t^{\text{pole}}, \rho_s) \quad \rho_s = \frac{2m_0}{\sqrt{s_{t\bar{t}+1\text{-jet}}}}$$

- Unfold R + extract m_t^{pole} using NLO calculation [2,3]
- Reconstruct tT system using kinematic χ^2 -fit

[1] arXiv:1507.01769, subm. to JHEP

- similar to $\ell+\text{jets}$ result

- Define extra jet:

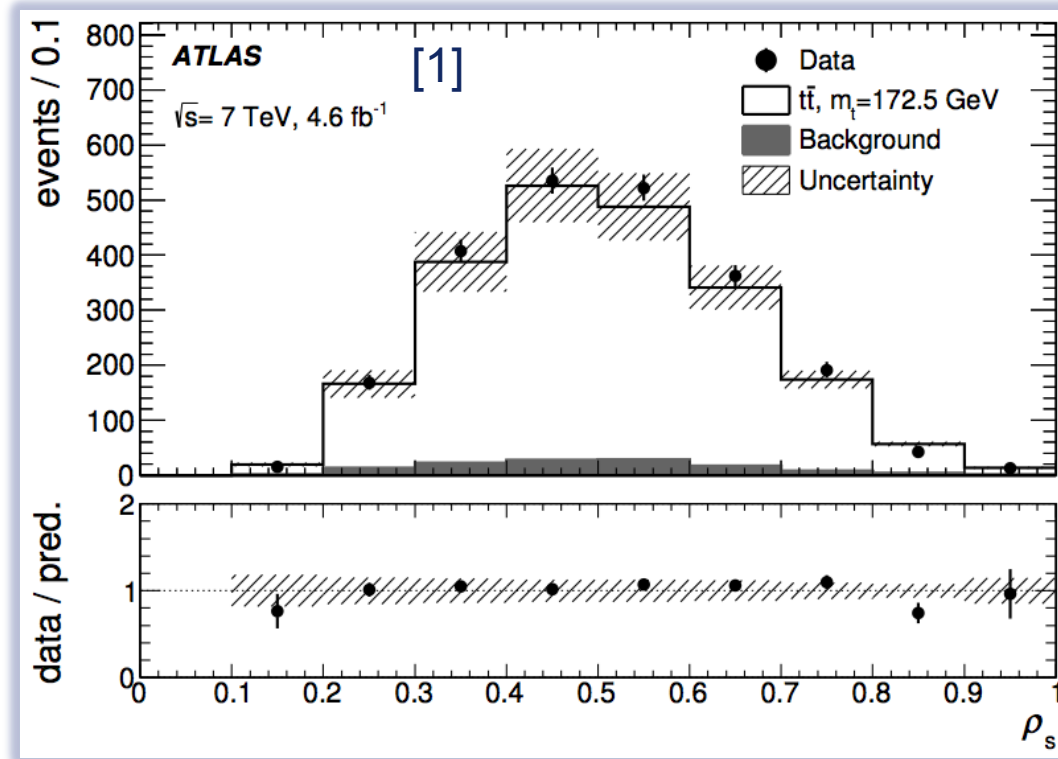
- not matched to tT system
- high $p_T > 50$ GeV
 - Enhance sensitivity

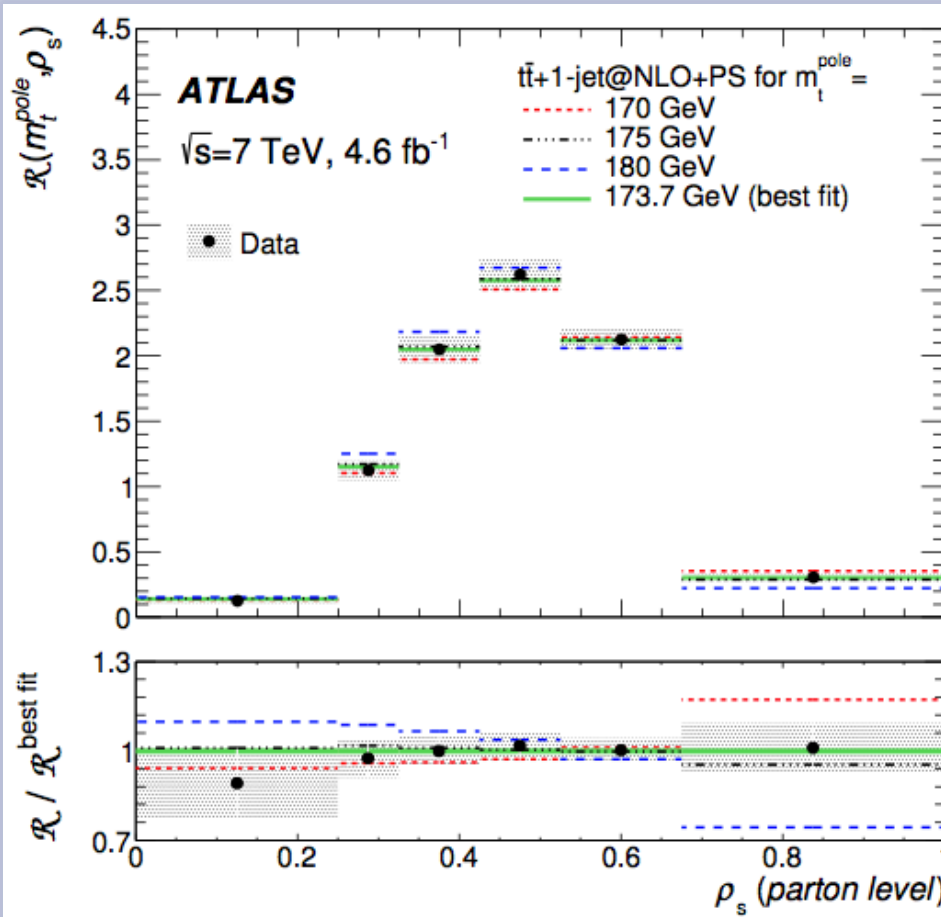
- Selection:

- similar to $\ell+\text{jets}$ result

[2] PRL 98 262002 (2007)

[3] EPJC 59 (2009) 625



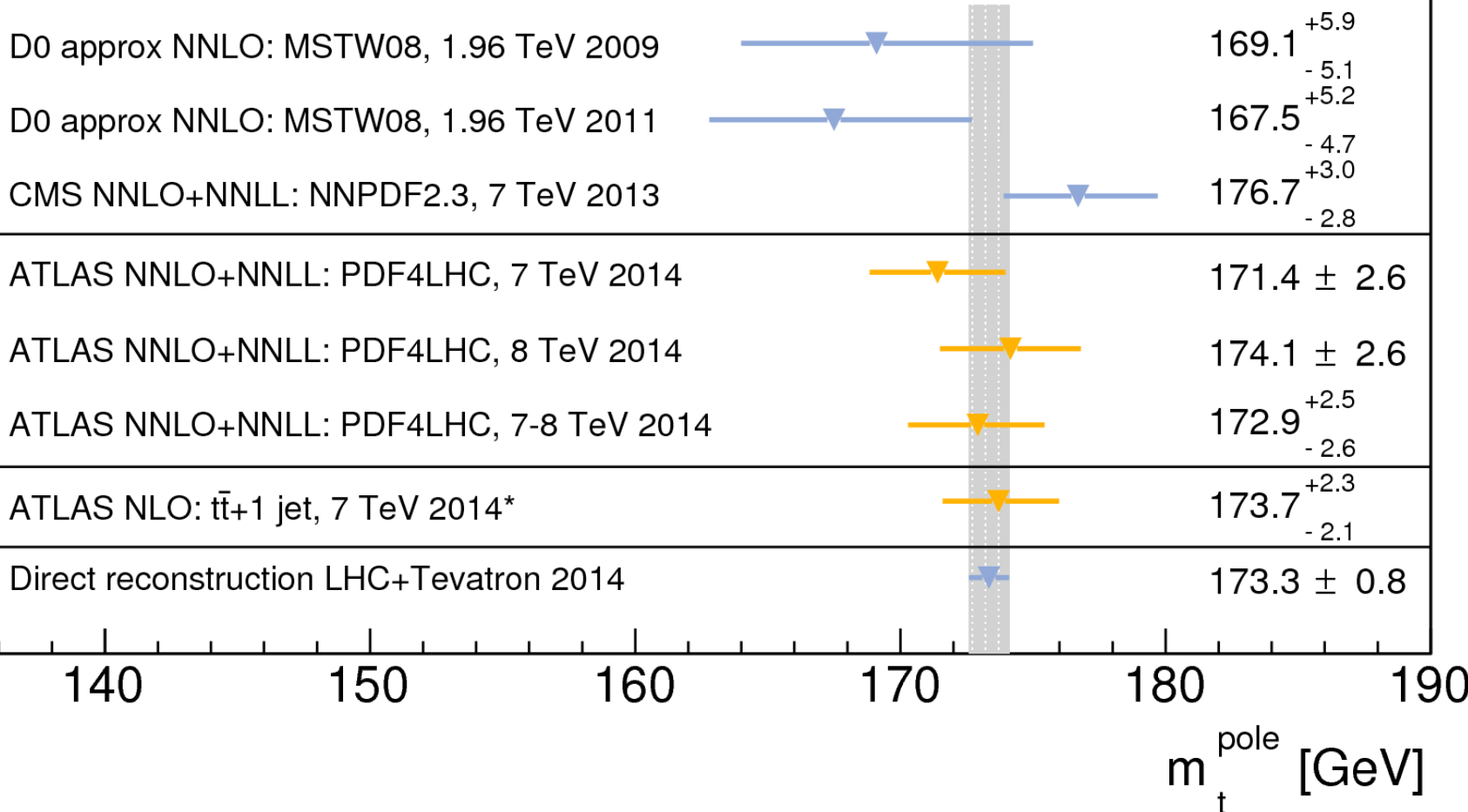


Dominant systematics (GeV):

- JES + b-quark JES (0.9)
 - Detector description
- Initial/final state radiat'n (0.7)
 - Affects extra jet production
- PDF in experiment (0.5)
 - Affects extra jet production
- Theory ($^{+1.0}_{-0.5}$)
 - Scale choice variation

$$m_t^{\text{pole}} = 173.7 \pm 1.5 \text{ (stat.)} \pm 1.4 \text{ (syst.)} {}^{+1.0}_{-0.5} \text{ (theory)} \text{ GeV,}$$

- World's most precise m_t^{pole} from σ_{tT+j}
 - precision comparable to direct methods: $\approx 1.3\%$!

**ATLAS Preliminary**Top quark pole mass determinations
compared to direct measurement



- A wealth of m_t results in the last 5 years:
 - Improved overall precision below sub-GeV level
 - LHC achieves similar precision on m_t as the Tevatron
- Precision of ATLAS flagship analysis 0.53%!
 - Combination of $\ell+jets$ and $\ell\ell$ channels with correlations
- Innovative techniques put in place at ATLAS
 - Complementary approaches (e.g. single top)
 - *In situ* calibration of the b quark JES
 - World's most precise extraction of m_t^{pole} from $\sigma_{tT+1\text{jet}}$
 - etc. etc.
- New results from ATLAS @ $\sqrt{s}=8 \text{ TeV}$
 - Substantial improvement in statistics (bJSF)
- New studies with large datasets @ $\sqrt{s}=13 \text{ TeV}$
 - Better constrain systematic uncertainties from data





GAME OVER

BONUS MATERIAL

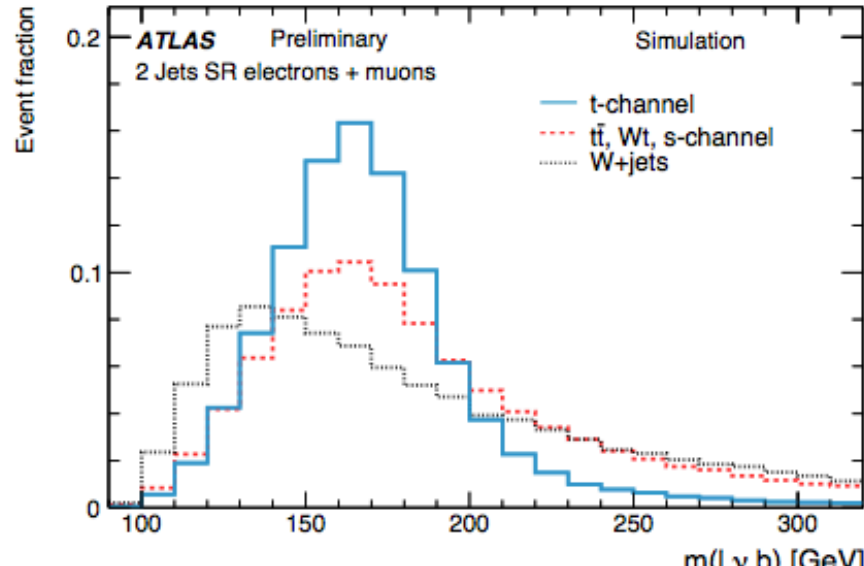


Single top

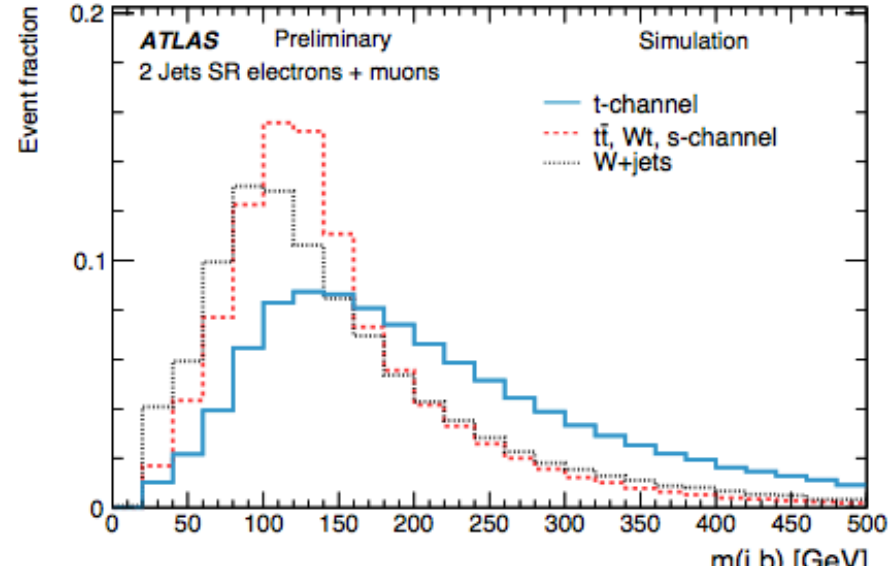


Table 1: Variables used as input to the neural network ordered by their importance, as estimated from the total correlation loss to the target caused by the removal of each specific variable.

Variable	loss of total correlation (%)	Variable	loss of total correlation (%)
$m(\ell\nu b)$	38	E_T^{miss}	7
$m(jb)$	31	$m_T(W)$	7
$m(\ell b)$	18	$\cos \theta(\ell, j)$ in the top quark rest frame	6
$ \eta(j) $	14	$p_T(W)$	3
$\eta(\ell\nu)$	13	$\eta(\ell\nu b)$	2
$H_T(\ell, \text{jets}, E_T^{\text{miss}})$	10	$\Delta R(\ell, \ell\nu b)$	1



(a)



(b)

Figure 2: Kinematic distributions of the two most significant variables in the signal region normalised to unit area for single-top t -channel and other processes: the invariant mass of the reconstructed top quark (a), invariant mass of the reconstructed light jet plus reconstructed b -tagged jet (b).

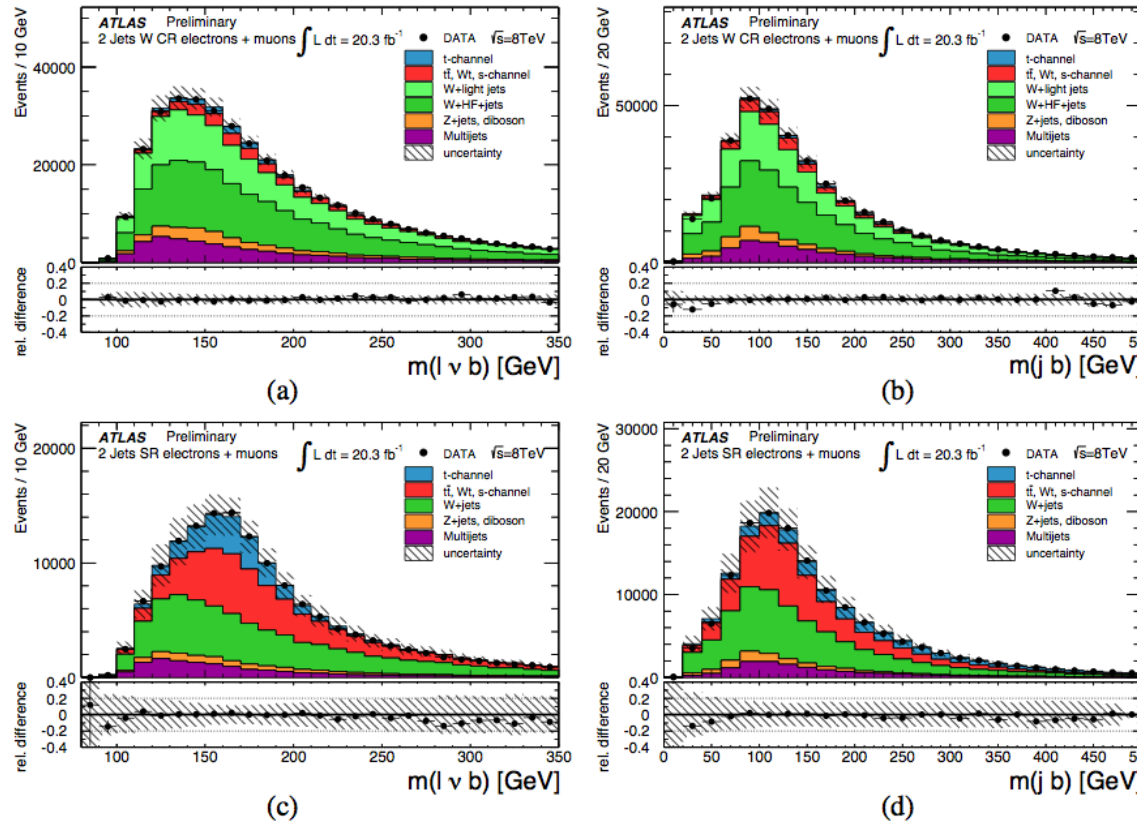
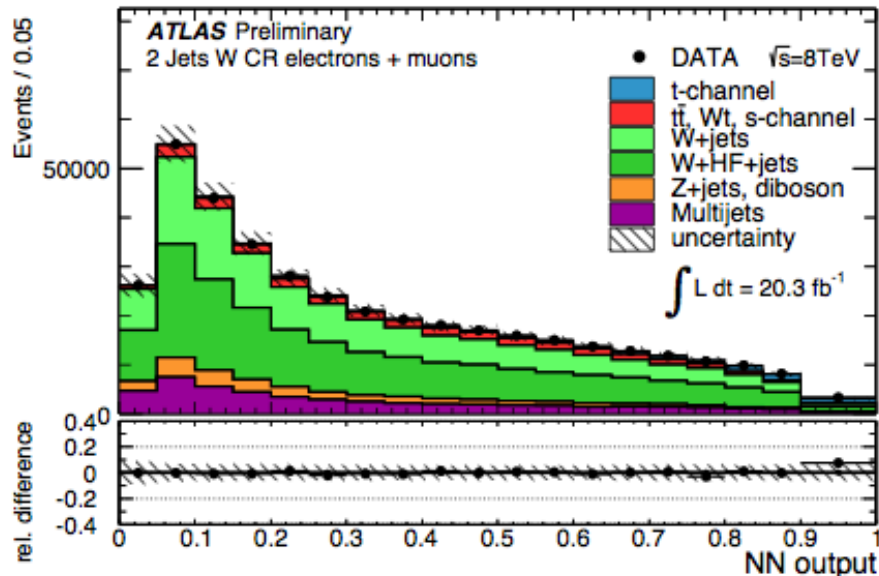
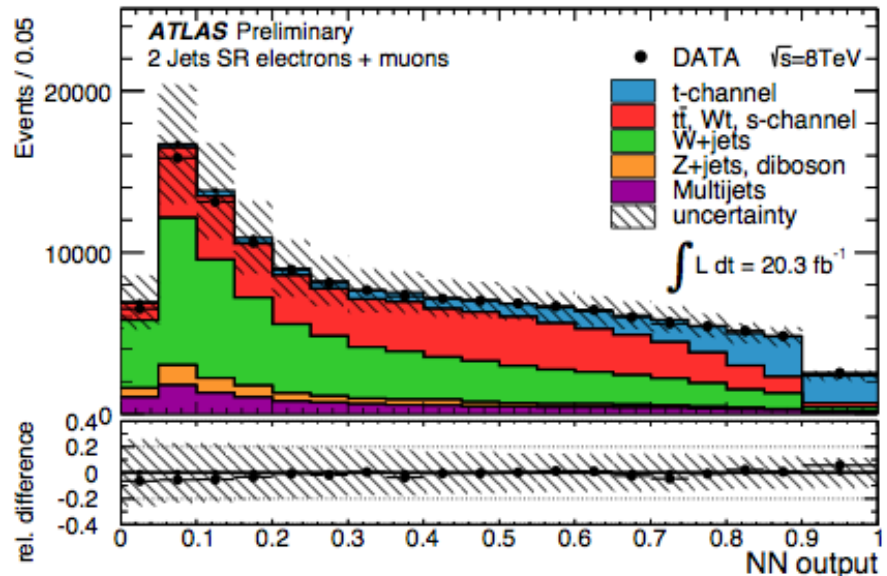


Figure 3: Simulated kinematic distributions of the two most significant variables in the construction of the neural network: the invariant mass of the reconstructed top quark (a, c), and the invariant mass of the reconstructed light-jet plus reconstructed b -tagged jet (b, d), shown in the control region (a, b) normalised to the result of the binned maximum likelihood fit used to determine the fraction of multijet events. The signal region shown in (c, d) is normalised to the number of expected events estimated in [49]. The relative difference $(O_i - E_i)/E_i$ between the observed O_i and expected E_i number of events in each bin i is shown in the lower histogram. The hatched bands indicate the statistical uncertainty from the simulated samples size and the systematic uncertainty on the multijet normalisation in the control region (a, b) and the statistical and W +jets normalisation uncertainties in the signal region in (c,d). The combined electron and muon channel is shown.



(a)



(b)

Figure 4: (a) Neural network output distribution in the control region normalised to the result of the binned maximum likelihood fit used to determine the fraction of multijet events. (b) Neural network output distribution in the signal region normalised to the number of expected events estimated in [49]. The relative difference $(O_i - E_i)/E_i$ between the observed O_i and expected E_i number of events in each bin i is shown in the lower histogram. The hatched band indicates the statistical uncertainty from the simulated samples size, the systematic uncertainty on the relative top normalisation and the systematic uncertainty on the multijet normalisation in (a) and statistical uncertainty and on the W +jets normalisation in (b).



Table 2: Predicted and observed event yields for the signal region (SR), for all selected events and events that fulfill a cut on the neural network (NN) output variable larger than 0.75. The multijet background estimation is derived from collision data based as discussed in Section 5 and the quoted uncertainty is the total uncertainty, dominated by the systematic uncertainty assignment of 50%. In the signal region SR ($NN > 0.75$), the data driven correction factors for the top processes are applied as well as the corresponding uncertainties. All the other expectations are derived using theoretical cross sections, and the corresponding uncertainties are theoretical. Since in both cases, a fit to data is performed, the expected and observed yields agree well.

Process	SR	SR ($NN > 0.75$)
t -channel	18100 ± 1800	9100 ± 1300
$t\bar{t}$, Wt , s -channel	54200 ± 4300	4940 ± 600
W +jets	51000 ± 28000	4090 ± 2200
Z +jets, diboson	6900 ± 1700	360 ± 90
Multijet	12200 ± 6100	950 ± 480
Total expectation	142000 ± 29000	19470 ± 2700
Data	143332	19833

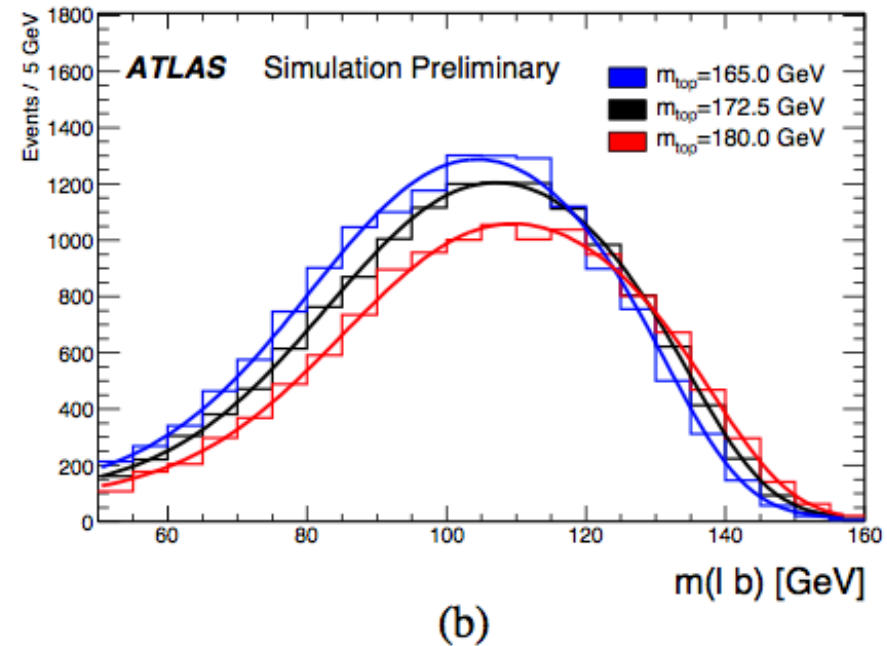
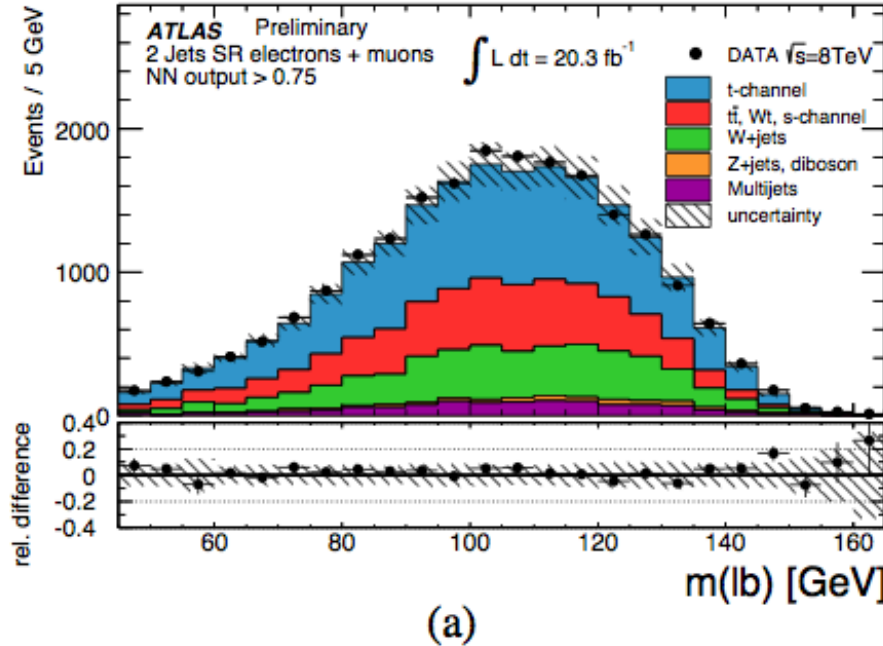


Figure 5: (a) Distributions of $m(\ell b)$ in the signal region for events with an output value of the neural network larger than 0.75. The data are compared to the MC predictions for signal and background. The signal MC processes assume $m_{\text{top}} = 172.5 \text{ GeV}$ and the expected distribution is normalised to the number of expected events estimated in [49]. The hatched bands indicate the statistical uncertainty from the simulated sample size and the systematic uncertainty on the W+jets normalisation. (b) Dependence of the $m(\ell b)$ distribution of all top quark processes on m_{top} for the signal MC samples generated with different input top quark masses, together with the signal probability density functions obtained from the parametrisation described in Section 7. The processes are normalized to the expectation for 20.3 fb^{-1} .



	Value [GeV]
Measured value	172.2
Statistical uncertainty	0.7
Jet energy scale	1.5
Jet energy resolution	< 0.1
Jet vertex fraction	< 0.1
Flavour tagging efficiency	0.3
Electron uncertainties	0.3
Muon uncertainties	0.1
Missing transverse momentum	0.2
W+jets normalisation	0.4
W+jets shape	0.3
Z+jets/diboson normalisation	0.2
Multijet normalisation	0.2
Multijet shape	0.3
Top normalisation	0.2
<i>t</i> -channel generator	< 0.1
<i>t</i> -channel hadronisation	0.7
<i>t</i> -channel colour reconnection	0.3
<i>t</i> -channel underlying event	< 0.1
<i>t</i> <i>t</i> , W <i>t</i> , and <i>s</i> -channel generator	0.2
<i>t</i> <i>t</i> hadronisation	< 0.1
<i>t</i> <i>t</i> colour reconnection	0.2
<i>t</i> <i>t</i> underlying event	0.1
<i>t</i> <i>t</i> ISR/FSR	0.2
Proton PDF	< 0.1
Simulation sample statistics	0.3
Total systematic uncertainty	2.0
Total uncertainty	2.1



all-had



Jet-based trigger

≥ 6 jets with $p_T > 30 \text{ GeV}$ and $|\eta| < 2.5$

≥ 5 jets with $p_T > 55 \text{ GeV}$ and $|\eta| < 2.5$

$\Delta R > 0.6$ between pairs of jets with $p_T > 30 \text{ GeV}$

Jet vertex fraction JVF > 0.75

Reject events w. isolated electrons with $E_T > 25 \text{ GeV}$

Reject events w. isolated muons with $p_T > 20 \text{ GeV}$

Exactly 2 b -tagged jets among the four leading jets

Missing transverse momentum significance

$E_T^{\text{miss}} [\text{GeV}] / \sqrt{H_T [\text{GeV}]} < 3$

Centrality $\mathcal{C} > 0.6$

$$\mathcal{C} = \frac{\sum_j^{\text{jets}} E_{T,j}}{\sqrt{\left(\sum_j^{\text{jets}} p_j\right)^2}}$$



	Δm_t (GeV)
Signal modelling	
Method calibration	0.42
Trigger	0.01
Signal MC generator	0.30
Hadronisation	0.50
Fast simulation	0.24
Colour reconnection	0.22
Underlying event	0.08
ISR and FSR	0.22
Proton PDF	0.09
Pile-up	0.02
Background modelling	Δm_t (GeV)
Multijet background	0.35
Jet measurements	Δm_t (GeV)
Jet energy scale (see Table 4)	0.51
b -jet energy scale	0.62
Jet energy resolution	0.01
Jet reconstruction efficiency	0.01
b -tag efficiency and mistag rate	0.17
Soft contributions to missing energy	0.02
JVF scale factors	0.02
Total systematic uncertainty	1.22

Table 4 Individual contributions to the systematic uncertainty of the top-quark mass due to uncertainties on the jet energy scale listed in Table 3

	Δm_t (GeV)
Statistics and method	0.09
Physics modelling	0.31
Detector description	0.36
Mixed detector and modelling	0.05
Single high- p_T particle	0.02
Relative non-closure in MC	0.04
Pile-up	0.03
Close-by jets	0.02
Flavour composition and response	0.10
Jet energy scale	0.51
b -jet energy scale	0.62

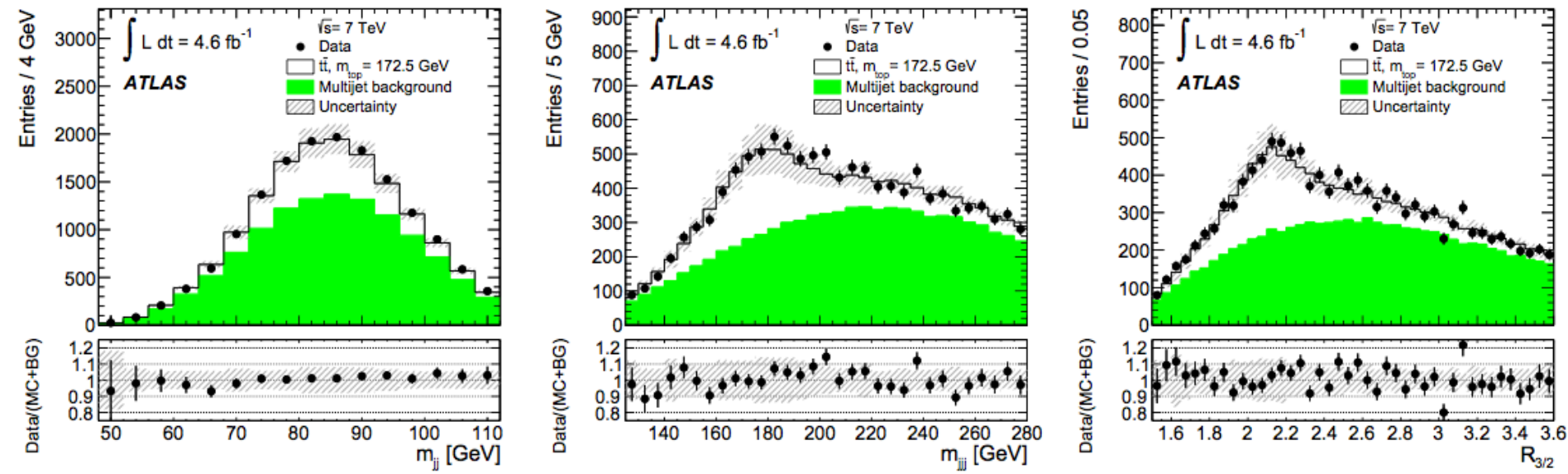


Fig. 2 Distributions of (left) dijet mass m_{jj} , (middle) three-jet mass m_{jjj} , and (right) ratio of three-jet mass to dijet mass $R_{3/2}$, measured in data and compared to expectations after applying all analysis event selection criteria (i.e. for region F). The shape and normalisation of the multijet background distributions (green shaded histograms) are calculated using Eq. (4). The distributions for the $t\bar{t}$ events (white histograms) are taken from the MC simulation using a top-quark mass

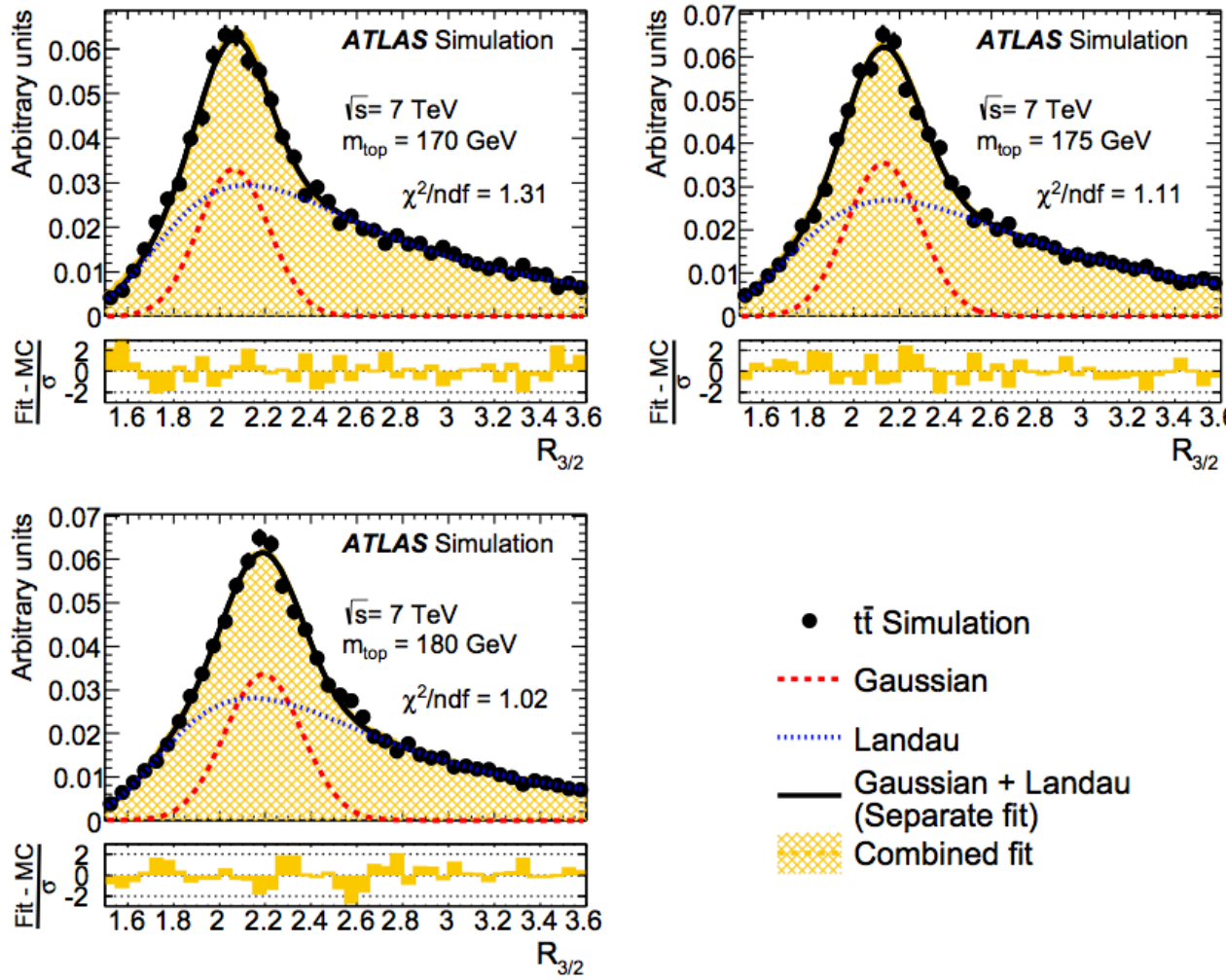
value of 172.5 GeV . The *insets* under the distributions show the ratio of data to the summed contributions of $t\bar{t}$ MC signal and modelled multijet background (see Sect. 4). The *error bars* represent the statistical uncertainties on the data. The *shaded bands* show the statistical and systematic (see Sect. 6) uncertainty on the expected signal and background distributions



Table 2 Event yields for the six regions, defined by the number of b -tagged jets and the transverse momentum of the sixth leading jet $p_T^{6\text{th jet}}$, are listed for data and $t\bar{t}$ simulation assuming $m_t = 172.5$ GeV with

statistical uncertainty. The $t\bar{t}$ fractions are derived from the observed numbers of events and their statistical uncertainties

b -Tagged jets	$p_T^{6\text{th jet}} \leq 30$ GeV			$p_T^{6\text{th jet}} > 30$ GeV		
	Region R	Data events N_R^{obs}	Signal MC events N_R^{sig}	Region R	Data events N_R^{obs}	Signal MC events N_R^{sig}
		Signal fraction	Signal fraction		Signal fraction	Signal fraction
0	A	93,732	306 ± 4	B	286,416	2607 ± 11
		0.33 ± 0.01 %			0.91 ± 0.01 %	
1	C	23,536	678 ± 5	D	77,301	5117 ± 14
		2.88 ± 0.04 %			6.62 ± 0.04 %	
2	E	4,532	399 ± 5	F	15,551	2582 ± 13
		8.80 ± 0.29 %			16.60 ± 0.27 %	



- $t\bar{t}$ Simulation
- Gaussian
- Landau
- Gaussian + Landau (Separate fit)
- Combined fit

Fig. 3 Templates for the $R_{3/2}$ distribution for $t\bar{t}$ MC simulation using top-quark mass values of 170.0, 175.0 and 180.0 GeV, respectively. For each top-quark mass, the $R_{3/2}$ distribution is fitted by the sum (black solid) of a Gaussian (red dashed) and Landau (blue dotted) function. Superimposed (orange cross-hatched) are the templates obtained from

a combined fit of all $R_{3/2}$ distributions using a linear dependence of parameters of the Gaussian and Landau functions on the top-quark mass value. The *insets* under the distributions show the difference $\text{Fit} - \text{MC}$ between the combined fit and the simulated $R_{3/2}$ histogram normalised to the statistical uncertainty σ of the corresponding $R_{3/2}$ bin



t +jets

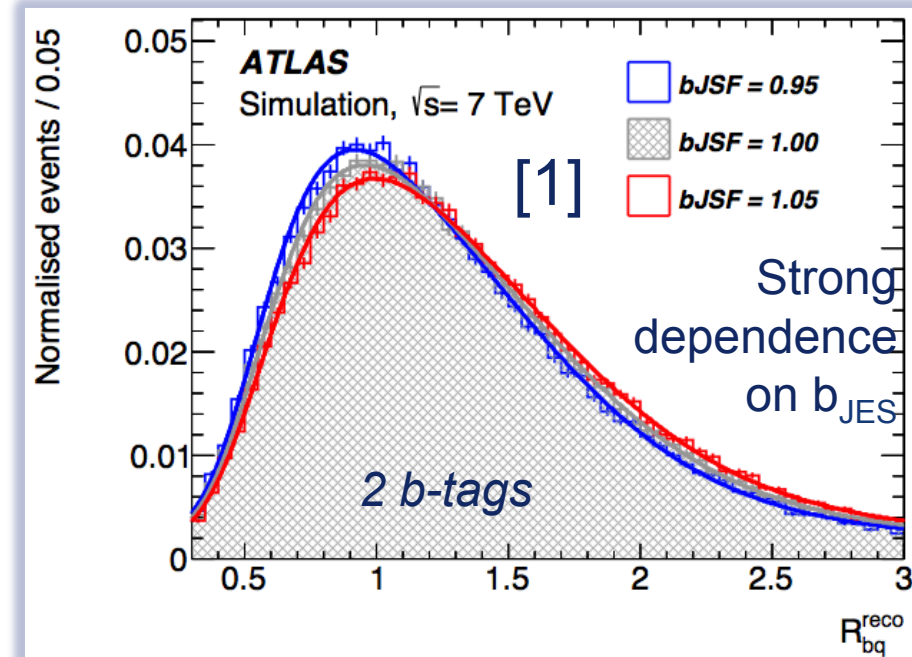


- Introduce R_{bq} variable to provide sensitivity to bJSF:

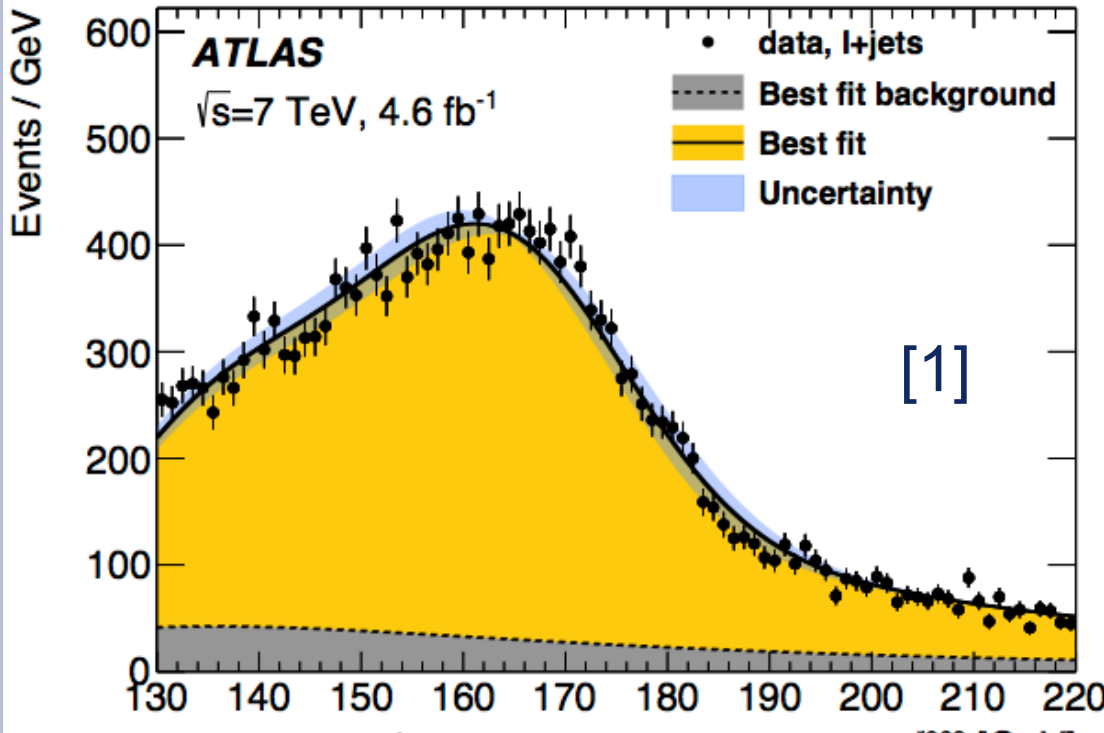
$$R_{bq}^{\text{reco},2\text{b}} = \frac{p_T^{b_{\text{had}}} + p_T^{b_{\text{lep}}}}{p_T^{W_{\text{jet}_1}} + p_T^{W_{\text{jet}_2}}}$$

$$R_{bq}^{\text{reco},1\text{b}} = \frac{p_T^{b_{\text{tag}}}}{(p_T^{W_{\text{jet}_1}} + p_T^{W_{\text{jet}_2}})/2}$$

(m_t , JSF, bJSF) are simultaneously extracted
→ Reduced systematic uncertainty
→ Increased statistical uncertainty:
 $\pm 0.23 (m_t) \text{ GeV}$
 $\pm 0.25 (k_{\text{JES}}) \text{ GeV}$
 $\pm 0.67 (b_{\text{JES}}) \text{ GeV}$
(m_t and k_{JES} fit only: $\pm 0.34 \text{ GeV}$)
 $\left. \right\} \pm 0.75 \text{ GeV}$



[1] ATLAS, subm. to EPJC, arXiv:1503.05427



[1] subm. to EPJC, arXiv:1503.05427

[2] CONF-2013-046 (cf. x-check analysis)

**In situ calibration of b_{JES} :
 very promising for the future!**

$$m_{\text{top}}^{\ell+\text{jets}} = 172.33 \pm 0.75 \text{ (stat + JSF + bJSF)} \pm 1.02 \text{ (syst)} \text{ GeV,}$$

relative uncertainty **0.73%**!

Statistics	0.75	0.35
– Stat. comp. (m_{top})	0.23	
– Stat. comp. (JSF)	0.25	
– Stat. comp. (bJSF)	0.67	
Method	0.11 ± 0.10	0.00
Signal MC	0.22 ± 0.21	1.30
Hadronisation	0.18 ± 0.12	0.96
ISR/FSR	0.32 ± 0.06	
Underlying event	0.15 ± 0.07	
Colour reconnection	0.11 ± 0.07	
PDF	0.25 ± 0.00	
$W/Z+\text{jets}$ norm	0.02 ± 0.00	
$W/Z+\text{jets}$ shape	0.29 ± 0.00	
NP/fake-lepton norm.	0.10 ± 0.00	
NP/fake-lepton shape	0.05 ± 0.00	
Jet energy scale	0.58 ± 0.11	0.92
b -jet energy scale	0.06 ± 0.03	
Jet resolution	0.22 ± 0.11	
Jet efficiency	0.12 ± 0.00	
Jet vertex fraction	0.01 ± 0.00	
b -tagging	0.50 ± 0.00	
$E_{\text{T}}^{\text{miss}}$	0.15 ± 0.04	
Leptons	0.04 ± 0.00	
Pile-up	0.02 ± 0.01	
	1.27 ± 0.33	

m_t+k_{JES} analysis [2]



	$m_{\text{top}}^{\ell+\text{jets}}$ [GeV]	$m_{\text{top}}^{\text{dil}}$ [GeV]	$m_{\text{top}}^{\text{comb}}$ [GeV]	ρ
Results	172.33	173.79	172.99	
Statistics	0.75	0.54	0.48	0
– Stat. comp. (m_{top})	0.23	0.54		
– Stat. comp. (JSF)	0.25	n/a		
– Stat. comp. (bJSF)	0.67	n/a		
Method	0.11 ± 0.10	0.09 ± 0.07	0.07	0
Signal MC	0.22 ± 0.21	0.26 ± 0.16	0.24	+1.00
Hadronisation	0.18 ± 0.12	0.53 ± 0.09	0.34	+1.00
ISR/FSR	0.32 ± 0.06	0.47 ± 0.05	0.04	-1.00
Underlying event	0.15 ± 0.07	0.05 ± 0.05	0.06	-1.00
Colour reconnection	0.11 ± 0.07	0.14 ± 0.05	0.01	-1.00
PDF	0.25 ± 0.00	0.11 ± 0.00	0.17	+0.57
W/Z+jets norm	0.02 ± 0.00	0.01 ± 0.00	0.02	+1.00
W/Z+jets shape	0.29 ± 0.00	0.00 ± 0.00	0.16	0
NP/fake-lepton norm.	0.10 ± 0.00	0.04 ± 0.00	0.07	+1.00
NP/fake-lepton shape	0.05 ± 0.00	0.01 ± 0.00	0.03	+0.23
Jet energy scale	0.58 ± 0.11	0.75 ± 0.08	0.41	-0.23
b-jet energy scale	0.06 ± 0.03	0.68 ± 0.02	0.34	+1.00
Jet resolution	0.22 ± 0.11	0.19 ± 0.04	0.03	-1.00
Jet efficiency	0.12 ± 0.00	0.07 ± 0.00	0.10	+1.00
Jet vertex fraction	0.01 ± 0.00	0.00 ± 0.00	0.00	-1.00
b-tagging	0.50 ± 0.00	0.07 ± 0.00	0.25	-0.77
$E_{\text{T}}^{\text{miss}}$	0.15 ± 0.04	0.04 ± 0.03	0.08	-0.15
Leptons	0.04 ± 0.00	0.13 ± 0.00	0.05	-0.34
Pile-up	0.02 ± 0.01	0.01 ± 0.00	0.01	0
Total	1.27 ± 0.33	1.41 ± 0.24	0.91	-0.07

substantial gains!

ℓ +jets: 1.27 GeV

dilep: 1.41 GeV

Comb'd: 0.91 GeV



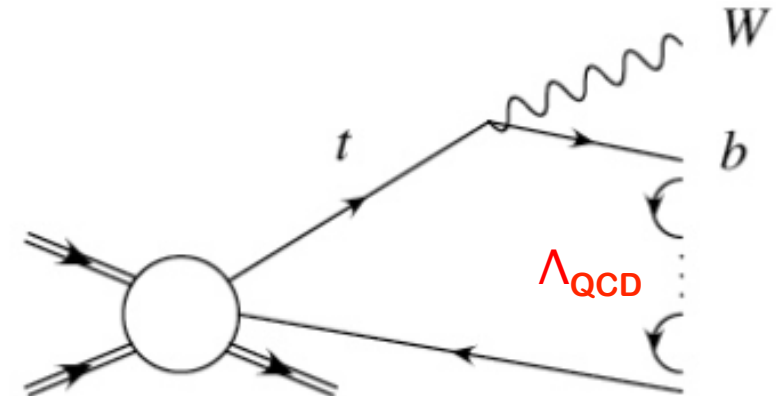
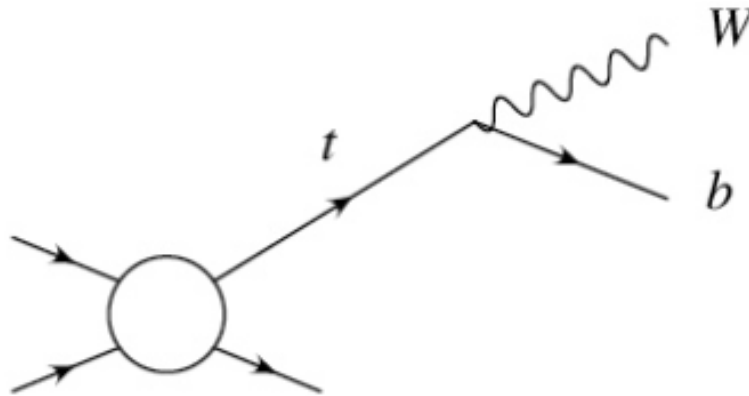
Alternative measurements



- m_t is not an observable but a SM parameter
 - \rightarrow inferred from its effect on kinematic observables
 - Not well-defined at LO
- Pole mass:
 - “Pole” in the top quark propagator:

$$\frac{i(p_t + m_t)}{p_t^2 - m_t^2} = \frac{i}{p_t - m_t}$$

- Not exact (hadronisation effects)
- Level of uncertainty: Λ_{QCD}





- Other mass definition schemes:
 - Modified minimal subtraction scheme ($\overline{\text{MS}}$)
 - Aka “running mass” $m_t(\mu_r)$
 - Absorb logarithmic corrections in $m_t(\mu_r)$ dependence through resummation
 - Better perturbative predictions
 - Can translate $\overline{\text{MS}}$ into pole mass at any fixed order pQCD
- Direct measurements shown so far:
 - m^{MC} (neither $\overline{\text{MS}}$, nor pole mass)
 - “Close” to pole mass (≈ 0.5 GeV)
 - True also for “NLO generators” like e.g. Powheg
 - → Top decay not simulated at NLO
- Alternative measurements (next slides):
 - Measure m_t in a well-defined scheme (typically pole)



$\sigma_{t\bar{T}+j}(m_t)$



Description	Value [GeV]	%
m_t^{pole}	173.71	
Statistical uncertainty	1.50	0.9
Scale variations	(+0.93, -0.44)	(+0.5, -0.3)
Proton PDF (theory) and α_s	0.21	0.1
Total theory systematic uncertainty	(+0.95, -0.49)	(+0.5, -0.3)
Jet energy scale (including b -jet energy scale)	0.94	0.5
Jet energy resolution	0.02	< 0.1
Jet reconstruction efficiency	0.05	< 0.1
b -tagging efficiency and mistag rate	0.17	0.1
Lepton uncertainties	0.07	< 0.1
Missing transverse momentum	0.02	0.1
MC statistics	0.13	< 0.1
Signal MC generator	0.28	0.2
Hadronization	0.33	0.2
ISR/FSR	0.72	0.4
Colour reconnection	0.14	< 0.1
Underlying event	0.25	0.1
Proton PDF (experimental)	0.54	0.3
Background	0.20	0.1
Total experimental systematic uncertainty	1.44	0.8
Total uncertainty	(+2.29, -2.14)	(+1.3, -1.2)



ρ_s interval	\mathcal{R}	$\sigma(\text{stat.}) \%$	$\sigma(\text{syst.}) \%$
0 to 0.25	0.126	12.8	7.1
0.25 to 0.325	1.122	6.6	4.5
0.325 to 0.425	2.049	5.0	3.5
0.425 to 0.525	2.622	4.6	2.1
0.525 to 0.675	2.125	4.1	3.1
0.675 to 1.0	0.302	8.2	8.1

Table 4: Measured values of the \mathcal{R} -distribution and its experimental uncertainties in percent. The statistical uncertainties are derived from the covariance matrix of eq. 9.

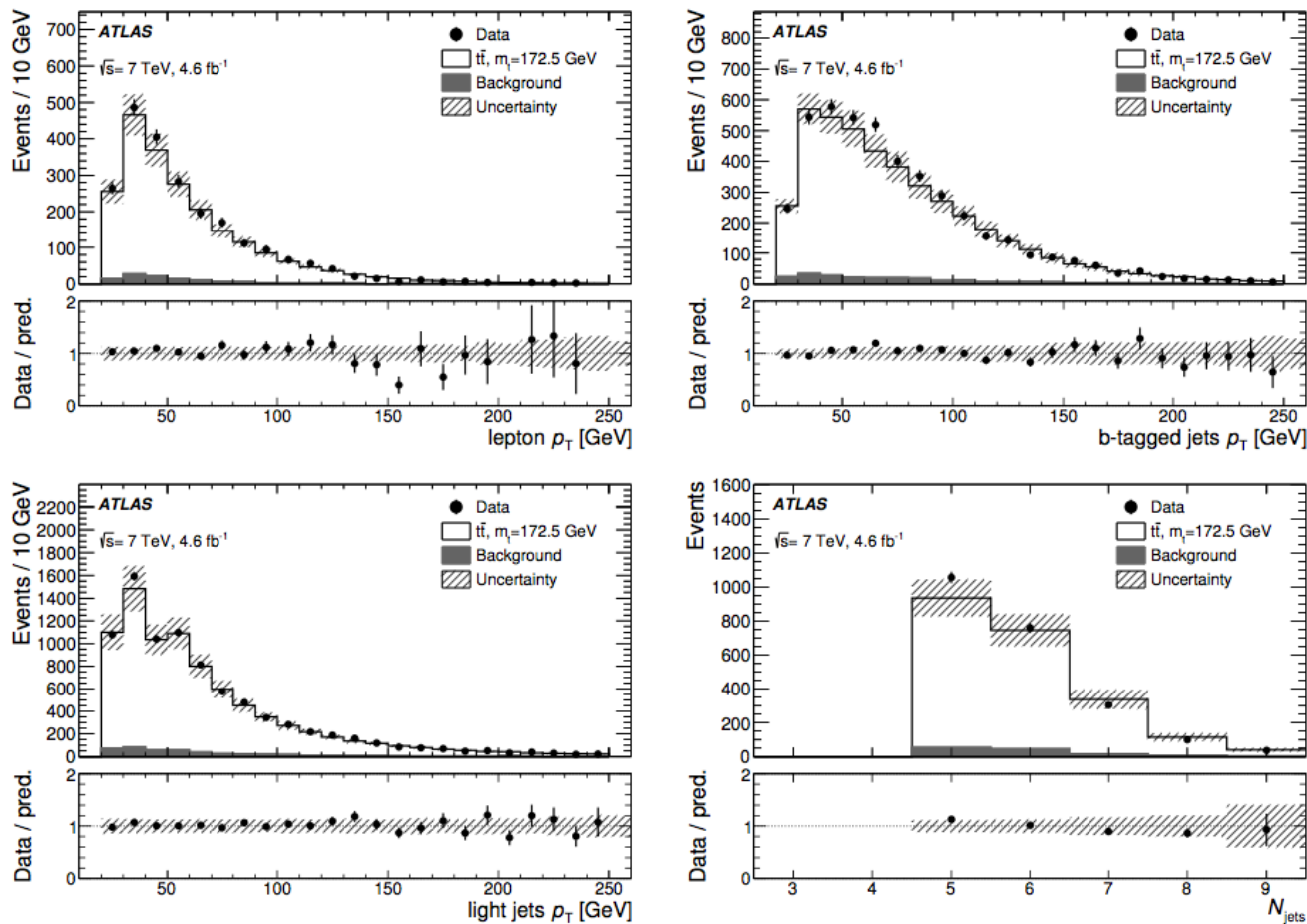


Figure 1: The data for various kinematic distributions (transverse momentum, p_T , of the lepton, p_T of all the b -tagged jets, p_T of all non- b -tagged jets and the total jet multiplicity) are compared to the nominal $t\bar{t}$ MC sample (POWHEG+PYTHIA) plus backgrounds after the final kinematic reconstruction of the $t\bar{t} + 1$ -jet events. The total background estimated in table 1 is shown in dark grey. The uncertainty band includes the total statistical and systematic uncertainties as described in section 8.

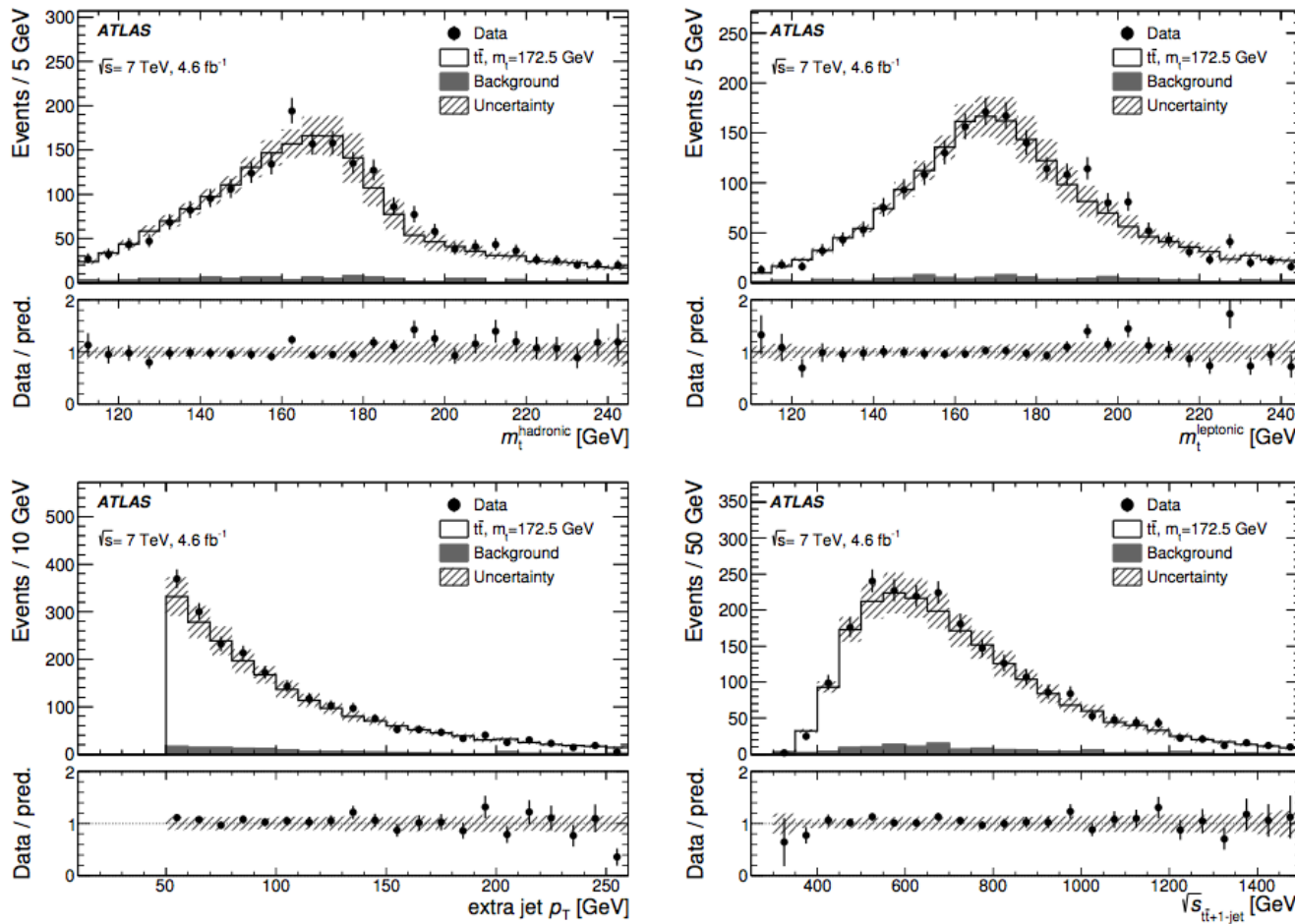


Figure 2: The data for various kinematic distributions (the reconstructed mass of the hadronically and leptonically decaying top-quark candidates, the p_T of the additional jet and the invariant mass of the $t\bar{t} + 1$ -jet system) are compared to the nominal $t\bar{t}$ MC sample (PowHEG+PYTHIA) plus backgrounds after the final kinematic reconstruction of the $t\bar{t} + 1$ -jet events. The total background estimated in table 1 is shown in dark grey. The uncertainty band includes the total statistical and systematic uncertainties as described in section 8.



	Events	Uncertainty
Signal ($t\bar{t}$, $m_t = 172.5$ GeV)	2050	\pm 320
$W+$ jets	31	\pm 16
$Z+$ jets	6	\pm 4
Single top ($m_t = 172.5$ GeV)	62	\pm 34
WW, ZZ, WZ	1	\pm 1
Misidentified and non-prompt leptons	22	\pm 13
Total Background	121	\pm 40
Total Predicted	2170	\pm 320
Data	2256	

Table 1: Event yields and their uncertainties after the reconstruction of the $t\bar{t} + 1$ -jet system. The quoted uncertainty values include the total statistical and systematic uncertainties as described in section 8.

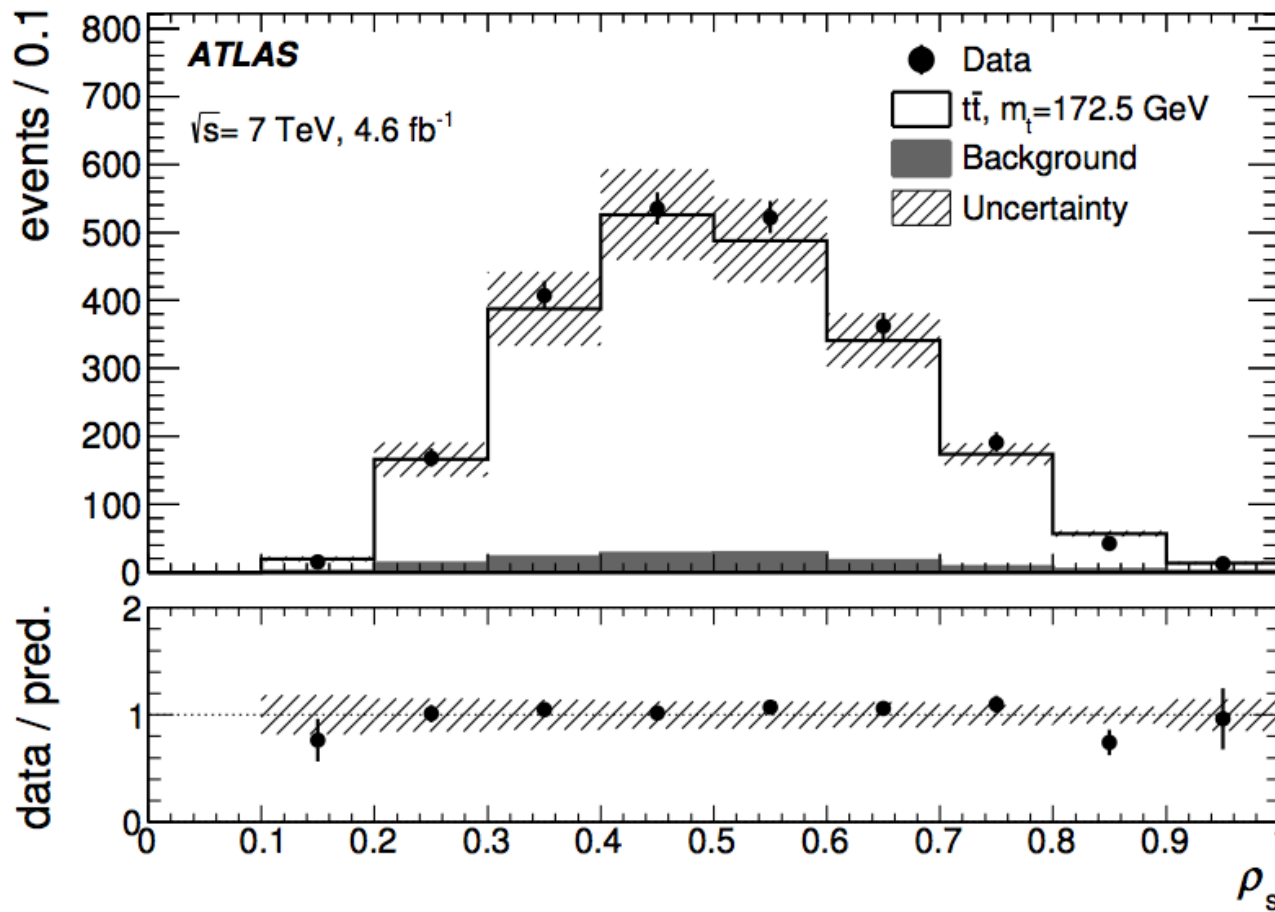


Figure 3: Number of reconstructed events as a function of ρ_s ($m_0 = 170$ GeV) related to the inverse of the invariant mass of the $t\bar{t} + 1\text{-jet}$ system. The data are compared to the nominal $t\bar{t}$ MC prediction (POWHEG+PYTHIA) plus backgrounds, which assumes a top-quark mass $m_t = 172.5$ GeV after the final kinematic reconstruction of the $t\bar{t} + 1\text{-jet}$ events. The backgrounds and the systematic uncertainties are estimated as in figure 1 and 2.

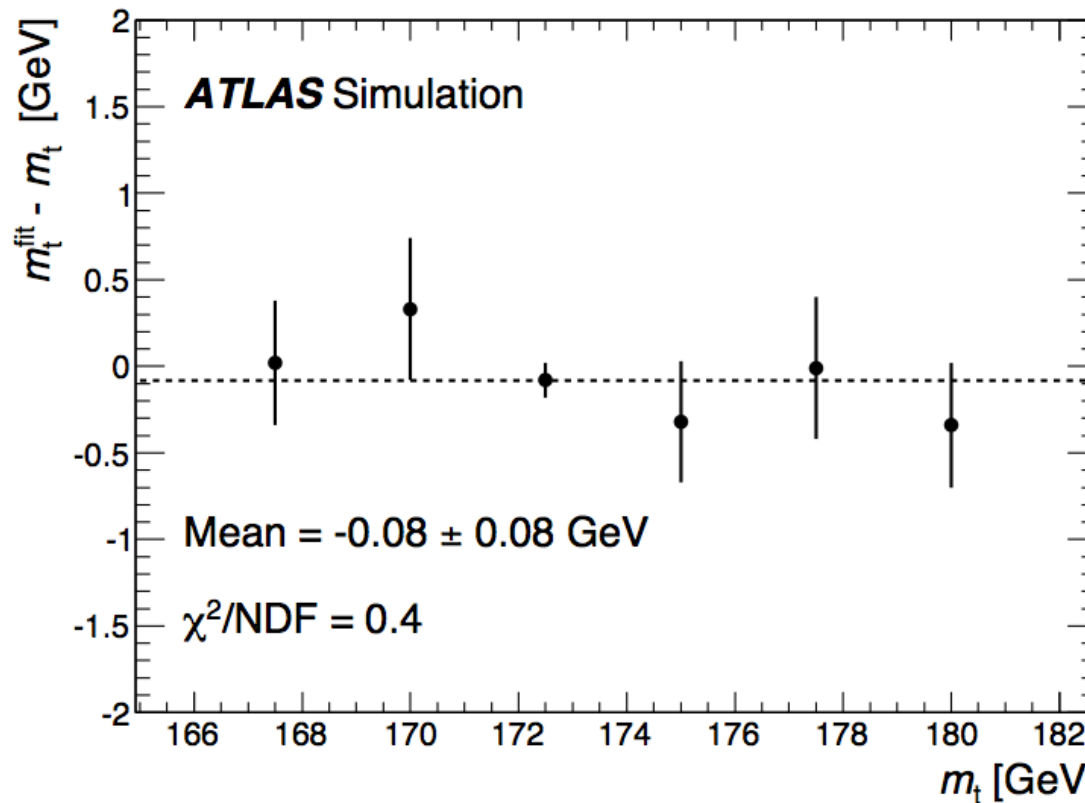
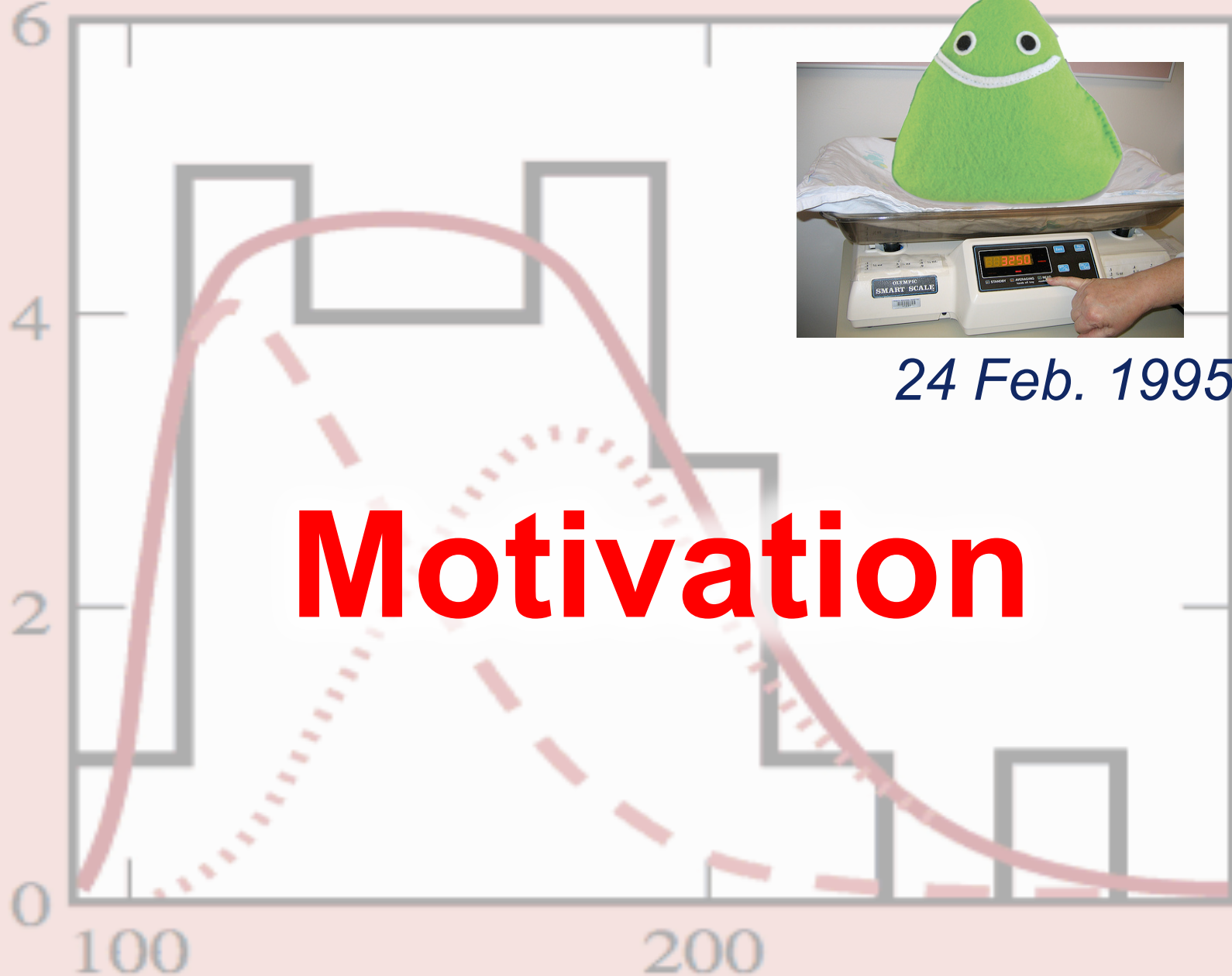


Figure 5: Difference between the fitted mass and the top-quark mass assumed in the generated $t\bar{t}$ MC predictions (Powheg+Pythia) including full detector simulation as a function of the input mass. The same unfolding procedure employed for data is performed in this study. The migration matrix and correction factors are defined for a fixed top-quark mass of $m_t = 172.5$ GeV. The fit is performed using the parameterised mass dependence of the theoretical predictions obtained from the MC samples. A fit to a straight line including the point at 172.5 GeV is performed. The obtained mean value and χ^2/NDF are shown.



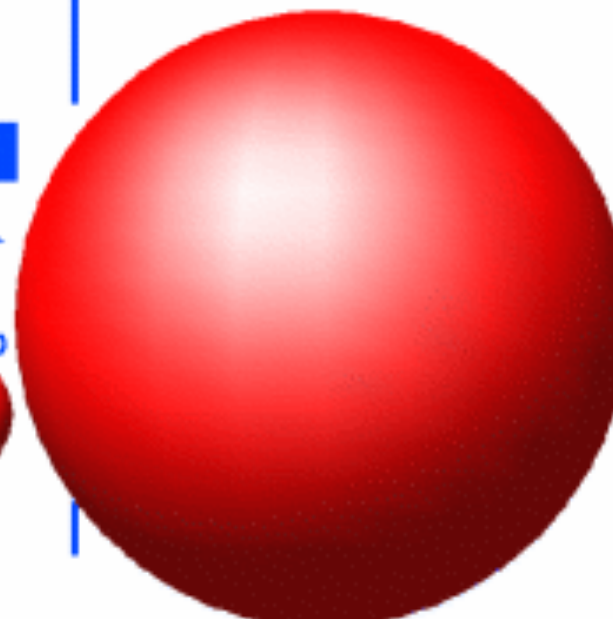
Events/(20 GeV/c²)



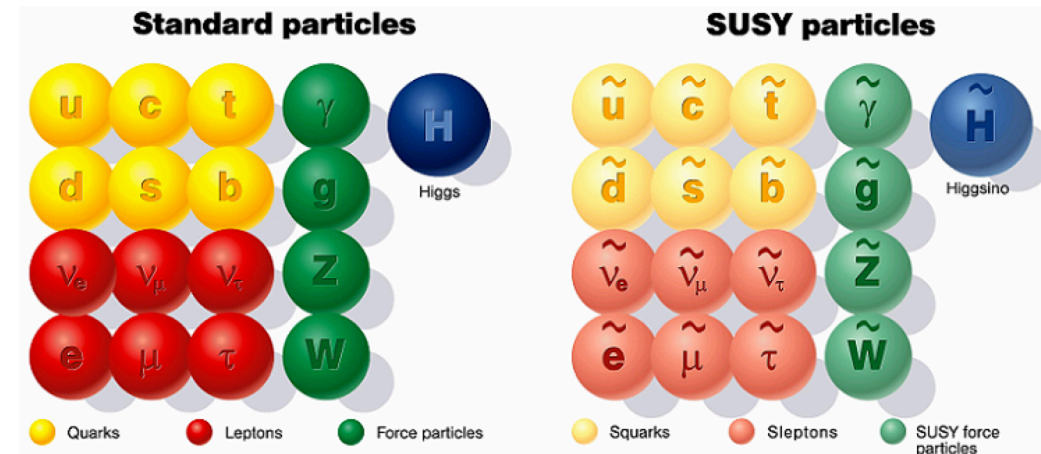
24 Feb. 1995



- The **top quark is special**:
 - **heaviest quark of the SM!**
 - **heaviest fundamental particle known**

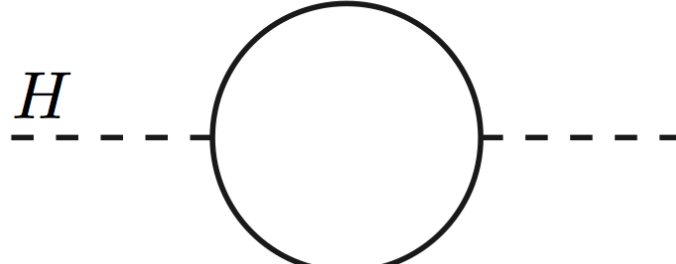


- **Special role in many new physics scenarios**
 - E.g. supersymmetry →



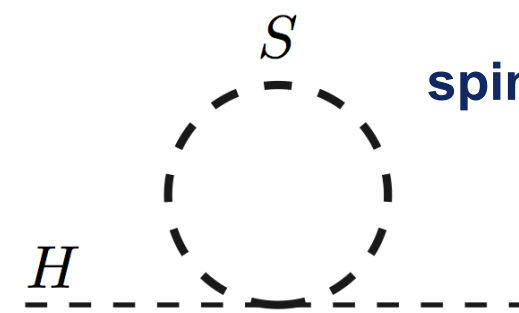
- Radiative corrections to M_{Higgs} :

spin-½ fermions



$$\Delta m_H^2 = -\frac{|\lambda_f|^2}{8\pi^2} \Lambda_{\text{UV}}^2 + \dots$$

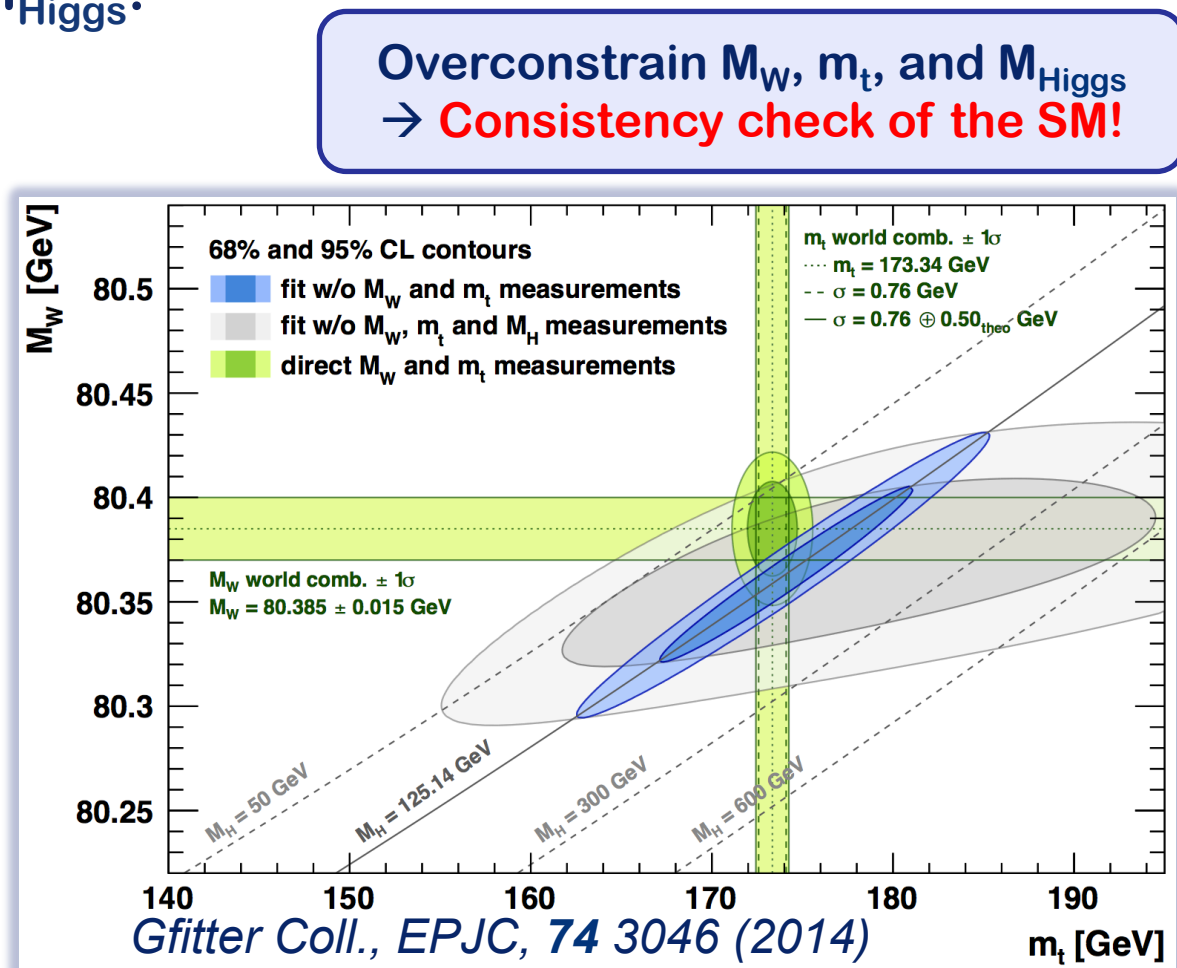
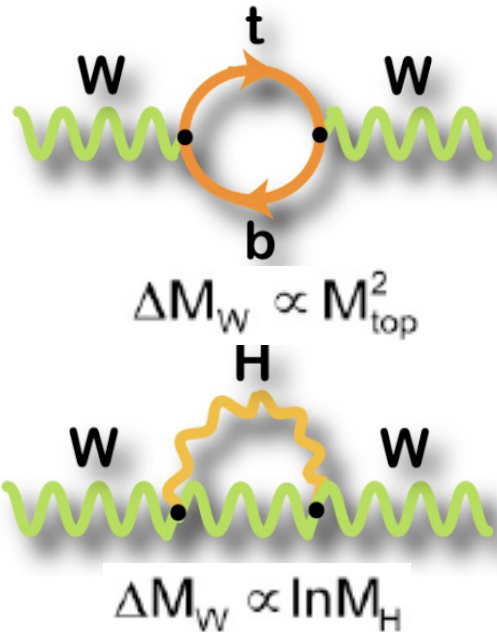
spin-0 bosons



$$\Delta m_H^2 = \frac{\lambda_S}{16\pi^2} \Lambda_{\text{UV}}^2 + \dots$$

- UV divergencies cancel if $|\lambda_f|^2 \approx \lambda_S$ or $m_t \approx M_t$

- **Special role in EW symmetry breaking?**
- M_W related to m_t & M_{Higgs} :



- The top quark mass is a fundamental SM parameter
- The fate of our Universe depends on m_t !

- $$\mathcal{L}_H = \left| \left(\partial_\mu - igW_\mu^a \tau^a - i\frac{g'}{2} B_\mu \right) \phi \right|^2 + \mu^2 \phi^\dagger \phi - \underline{\lambda(\phi^\dagger \phi)^2},$$

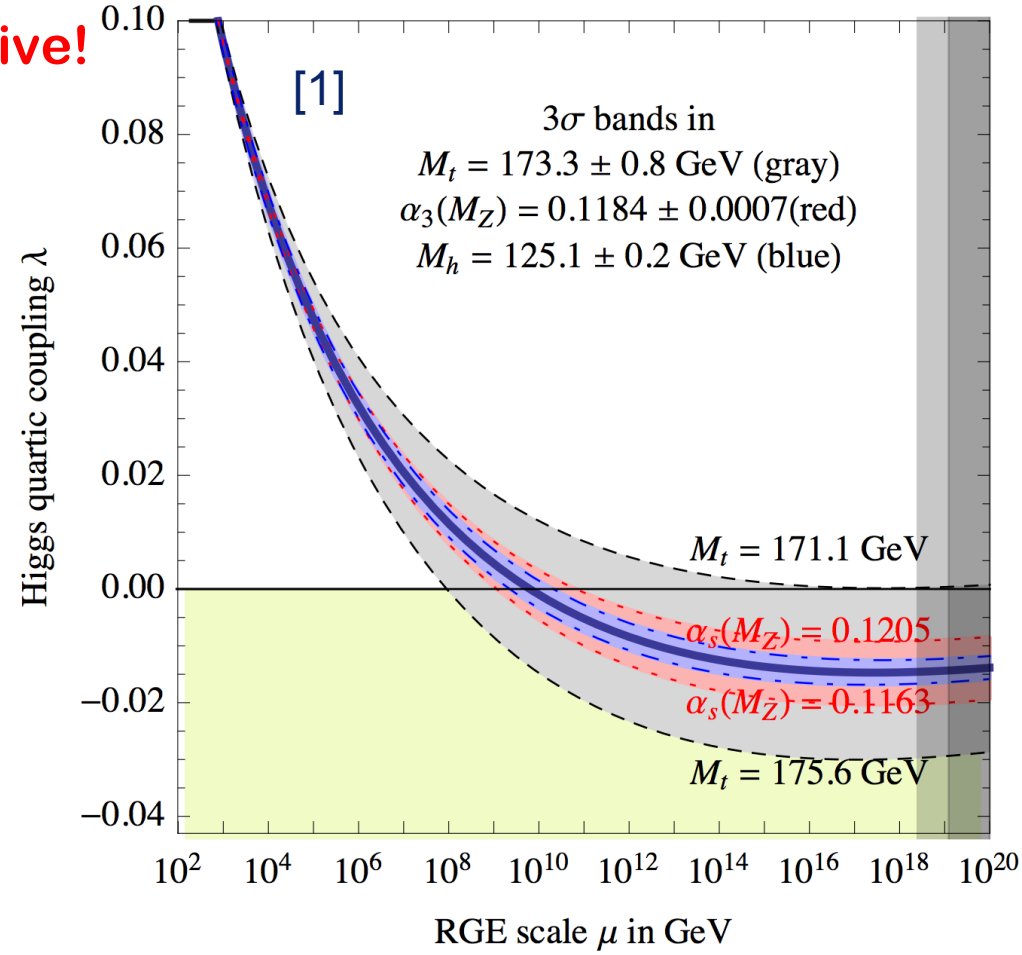
- Mexican hat only if $\lambda > 0$!

(poles flap down otherwise)



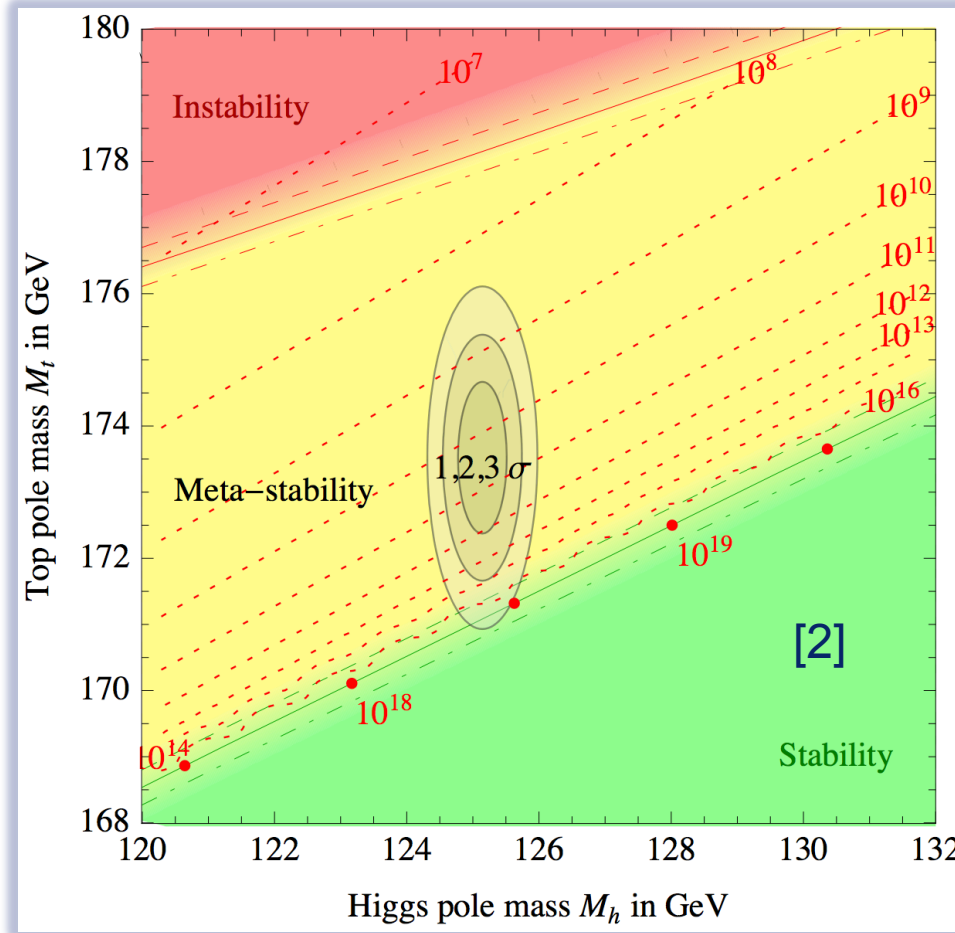


- λ receives **radiative corrections** from all SM particles
→ mostly from the top quark!
 - Evolve corrections to Planck scale:
 - λ should remain positive!



[1] Degrassi et al.,
[arXiv:1205.6497v4 \[hep-ph\]](https://arxiv.org/abs/1205.6497v4)

- Take world average values for m_t and M_{higgs} [1]:
 - Our universe is metastable [2]
 - → Exciting hints to new phenomena beyond the SM!



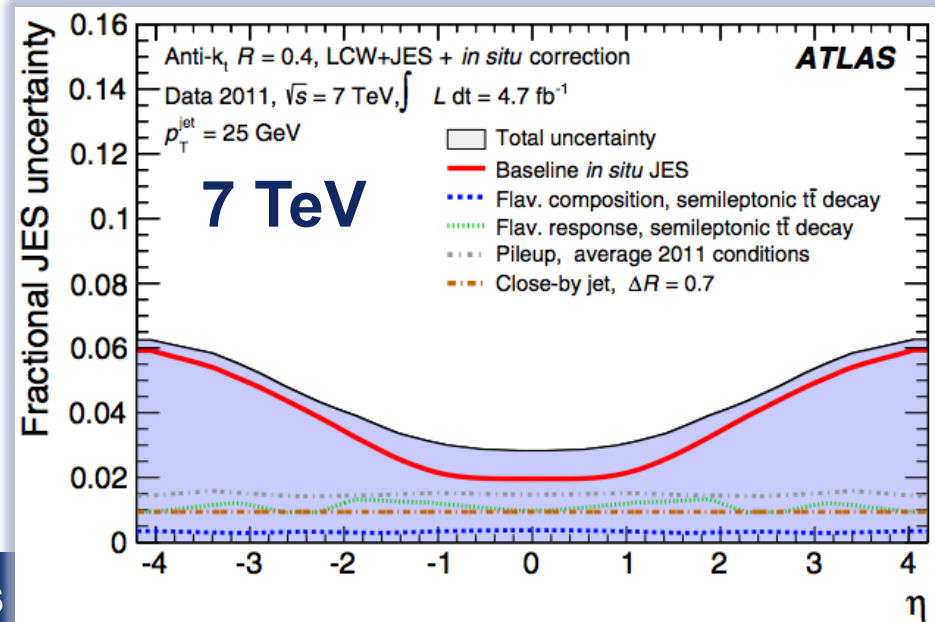
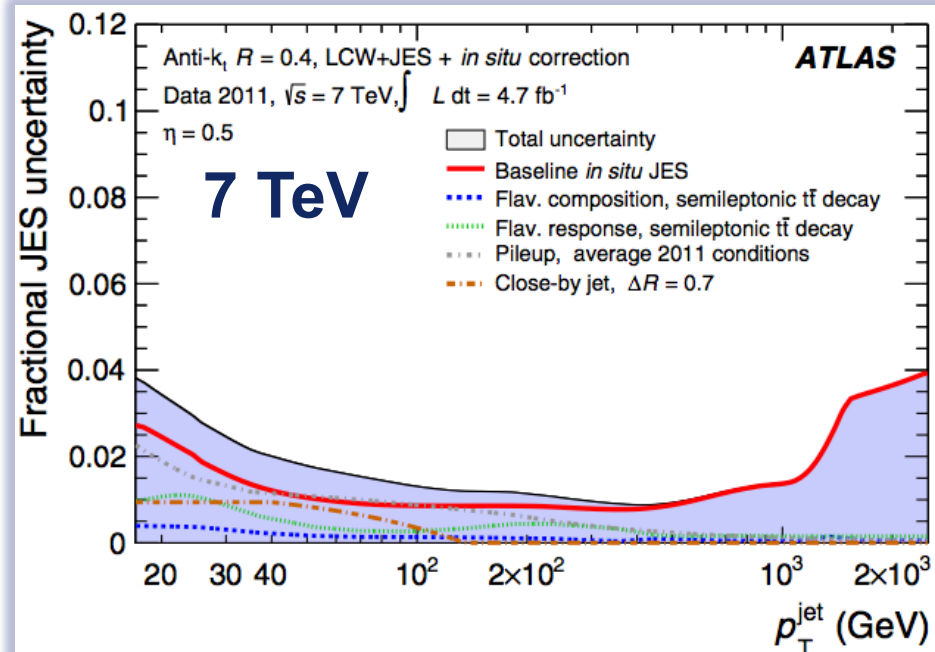
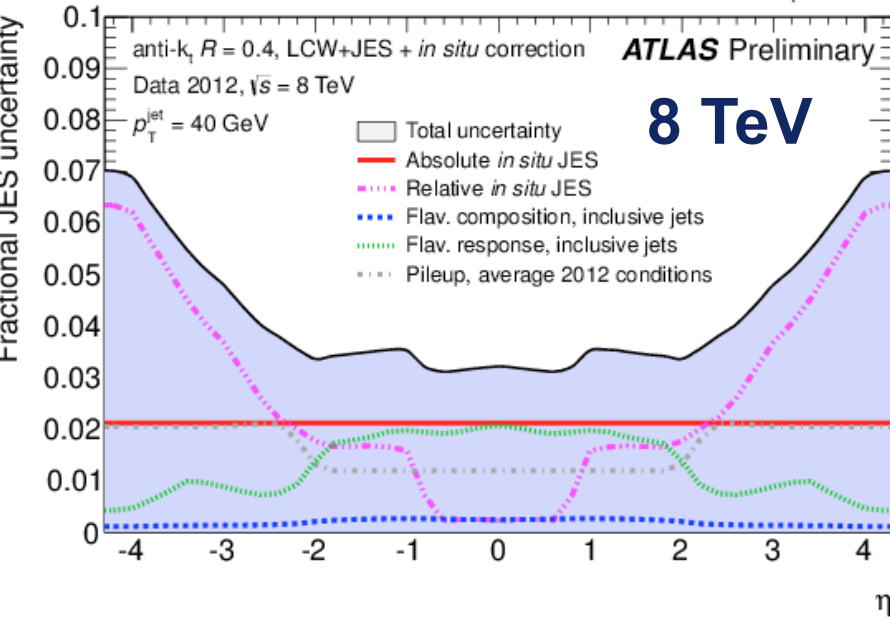
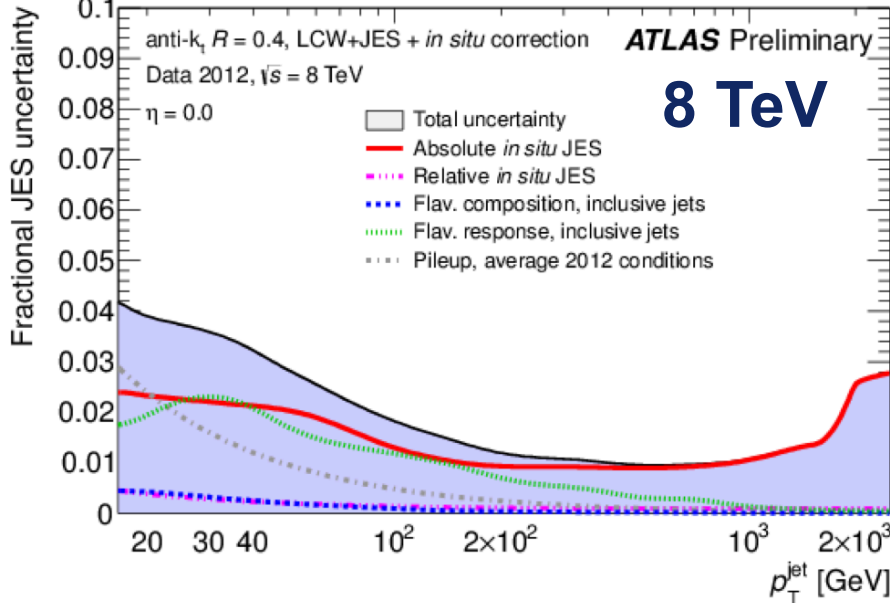
[1] ATLAS, CDF, CMS, DØ,
arXiv:1403.4427 [hep-ex]

[2] Degrassi et al.,
arXiv:1205.6497v4 [hep-ph]

The calculation includes NNLO effects,
RG equation at NNNLO

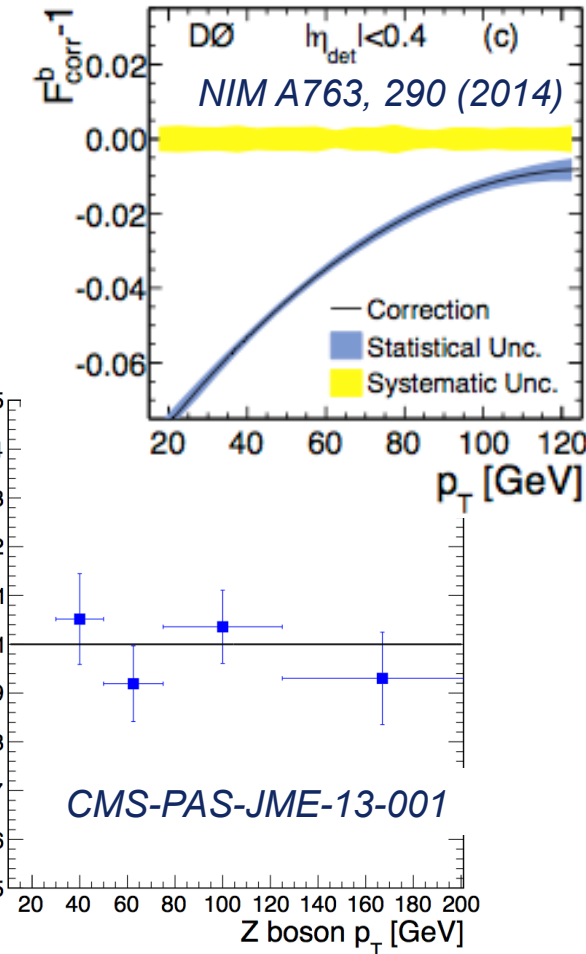
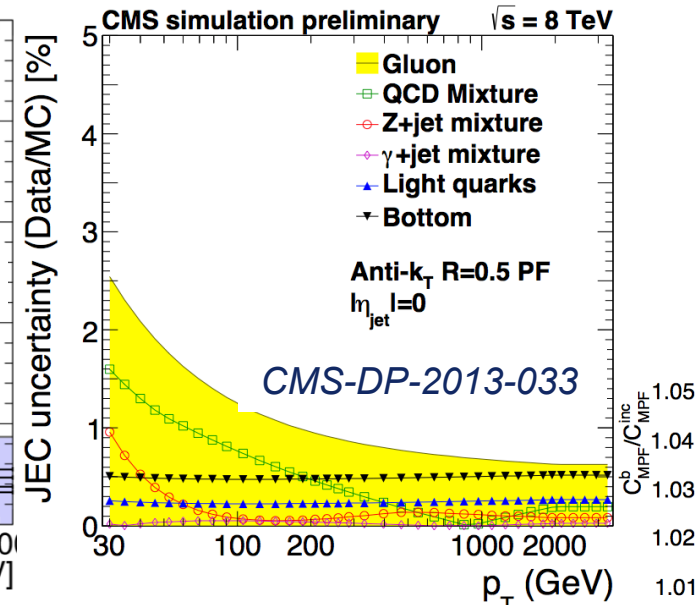
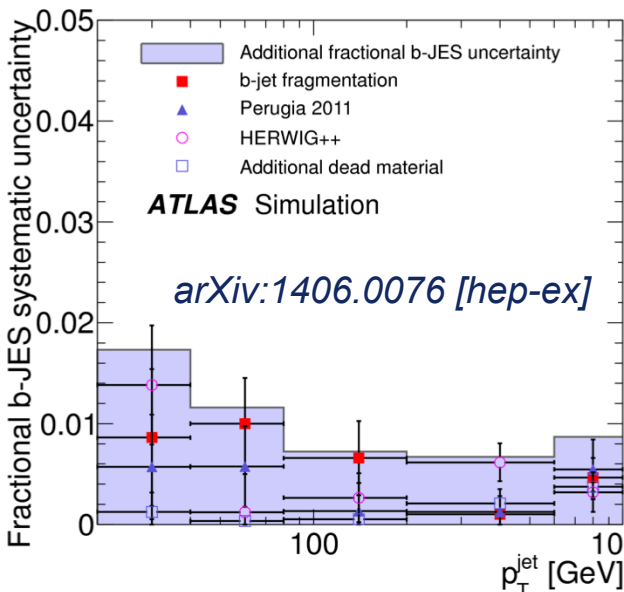


Experimental Uncert.



Flavour-dependence of JES calibration

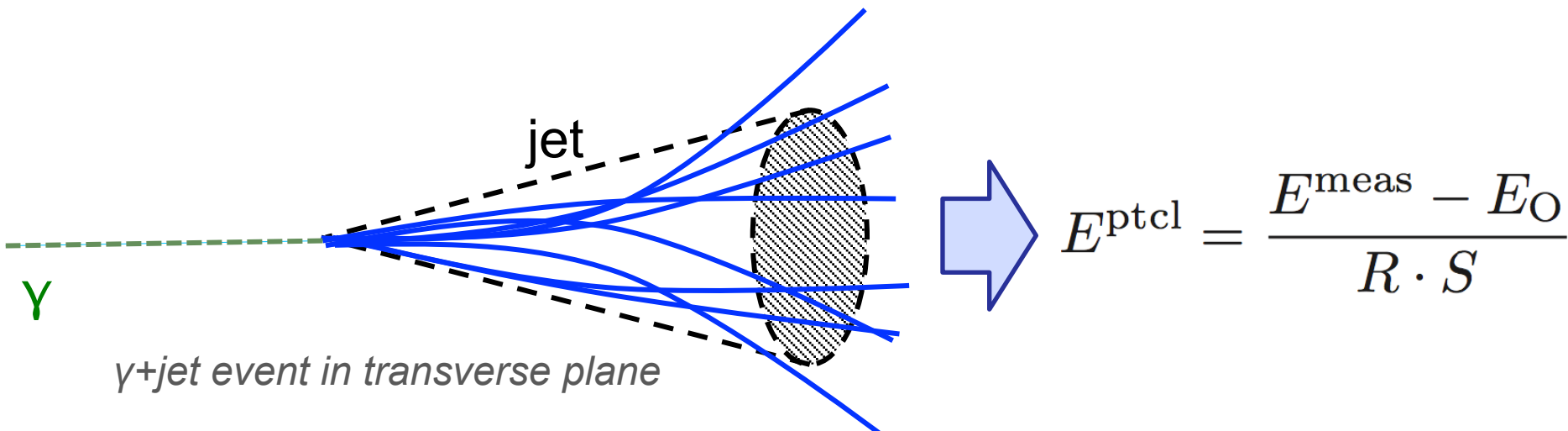
- Typically, estimate the uncertainty on the difference between b quark JES and standard JES by comparing fragmentation and parton shower models



*Cross-check
using $Z+b$ events*



- Generic procedure to calibrate jet energies:
 - 1) Calibrate EM energy scale with SM candles, i.e. $Z \rightarrow e^+e^-$
 - Central (well instrumented) region for **absolute** calibration
 - 2) Correct EM energy scale for e to that of γ
 - 3) $\gamma + \text{jet}$ events to calibrate major JES components
 - Basic idea: momentum balance in transverse plane

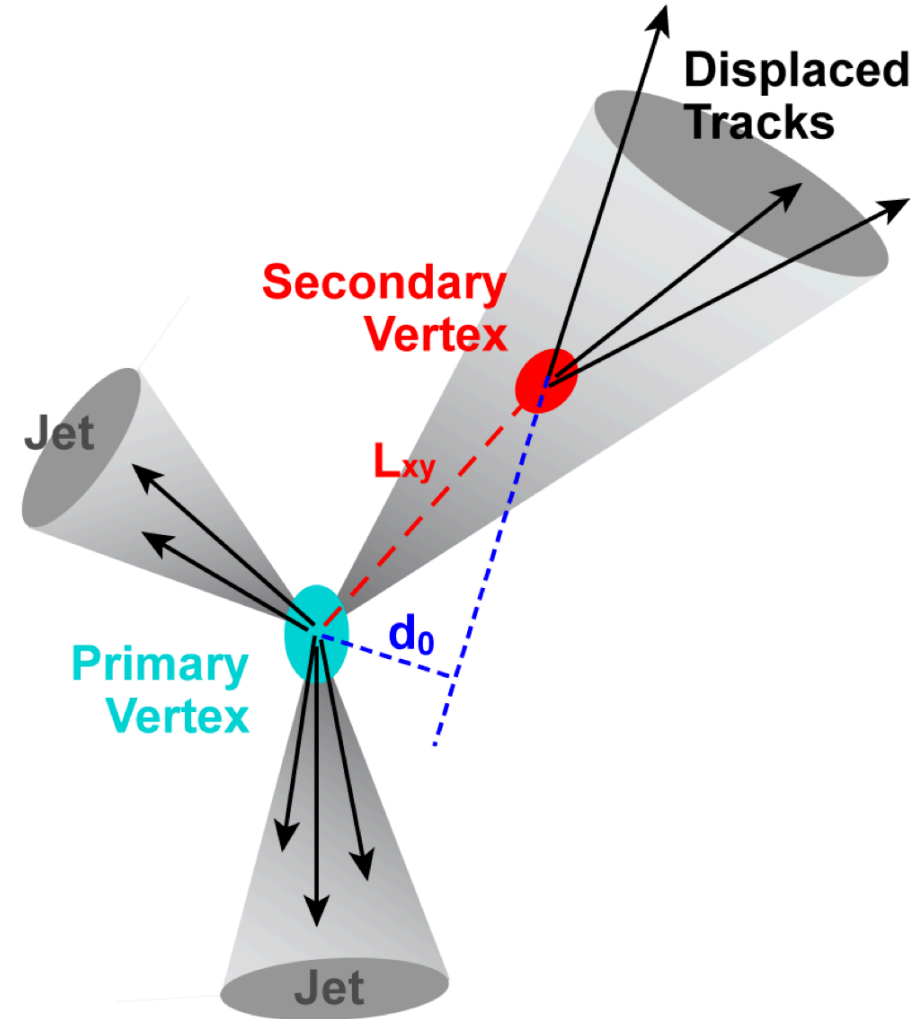


$\gamma + \text{jet}$ event in transverse plane

- Alternatively use $Z + \text{jet}$ events to calibrate JES
- Use $\gamma + \text{jet}$, $Z + \text{jet}$, and dijets to extend calibration in p_T, η

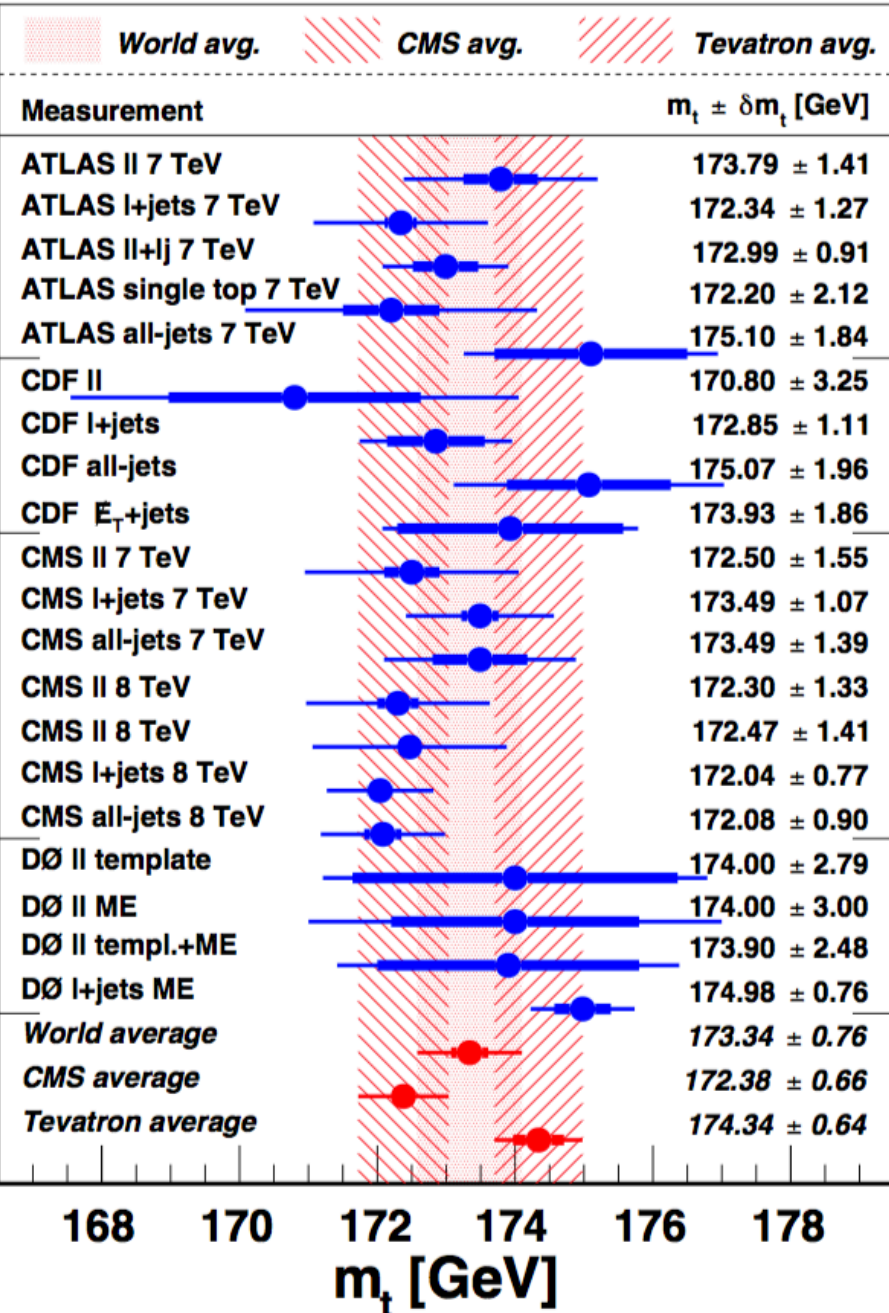


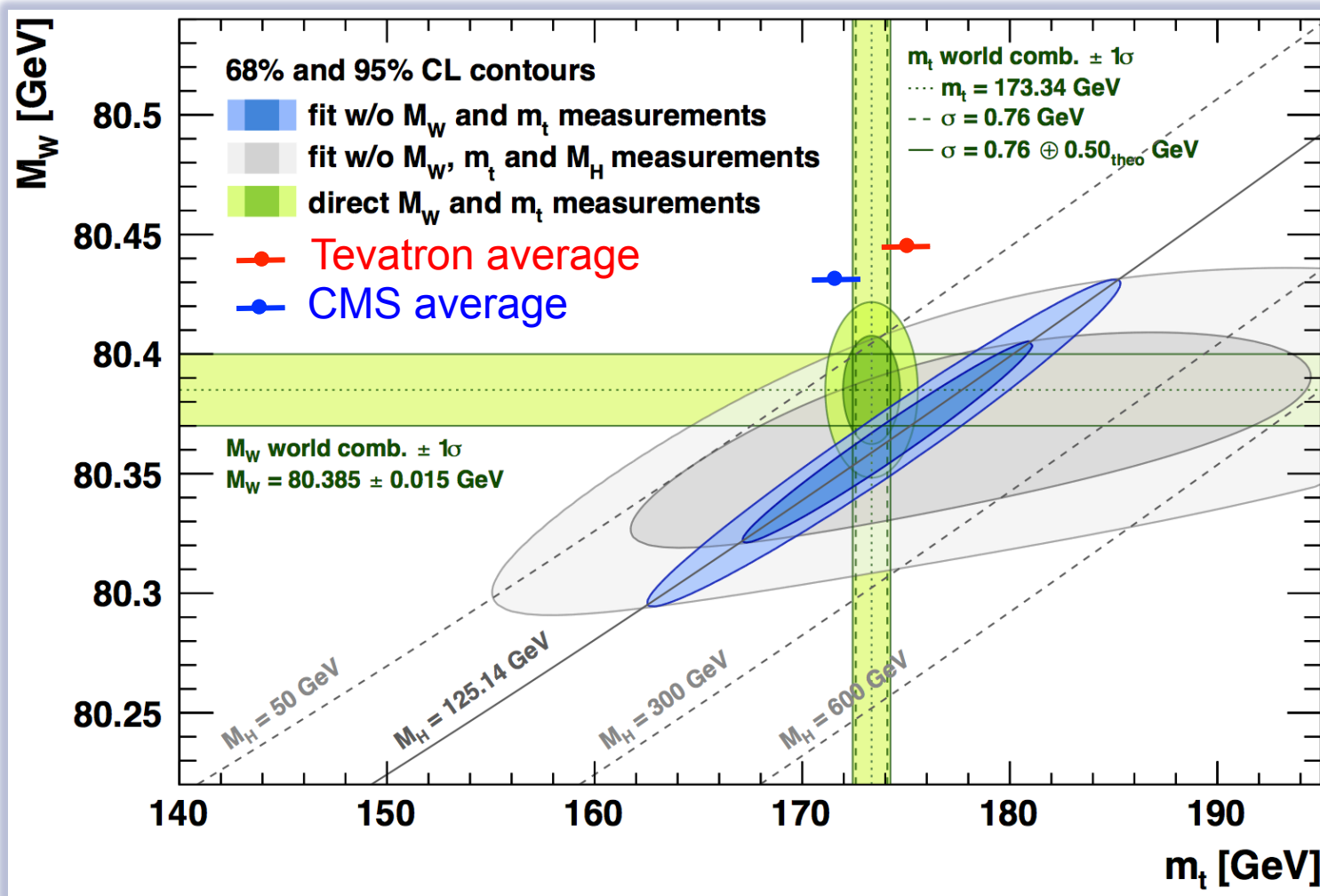
- 2 b quark jets in each tT event at Born level
 - → Separate signal from background
- Identify b quark jets:
 - Existence of a displaced secondary vertex
 - Impact parameters d_0 of tracks associated with the secondary vertex
 - Mass of the secondary vertex
 - Etc.





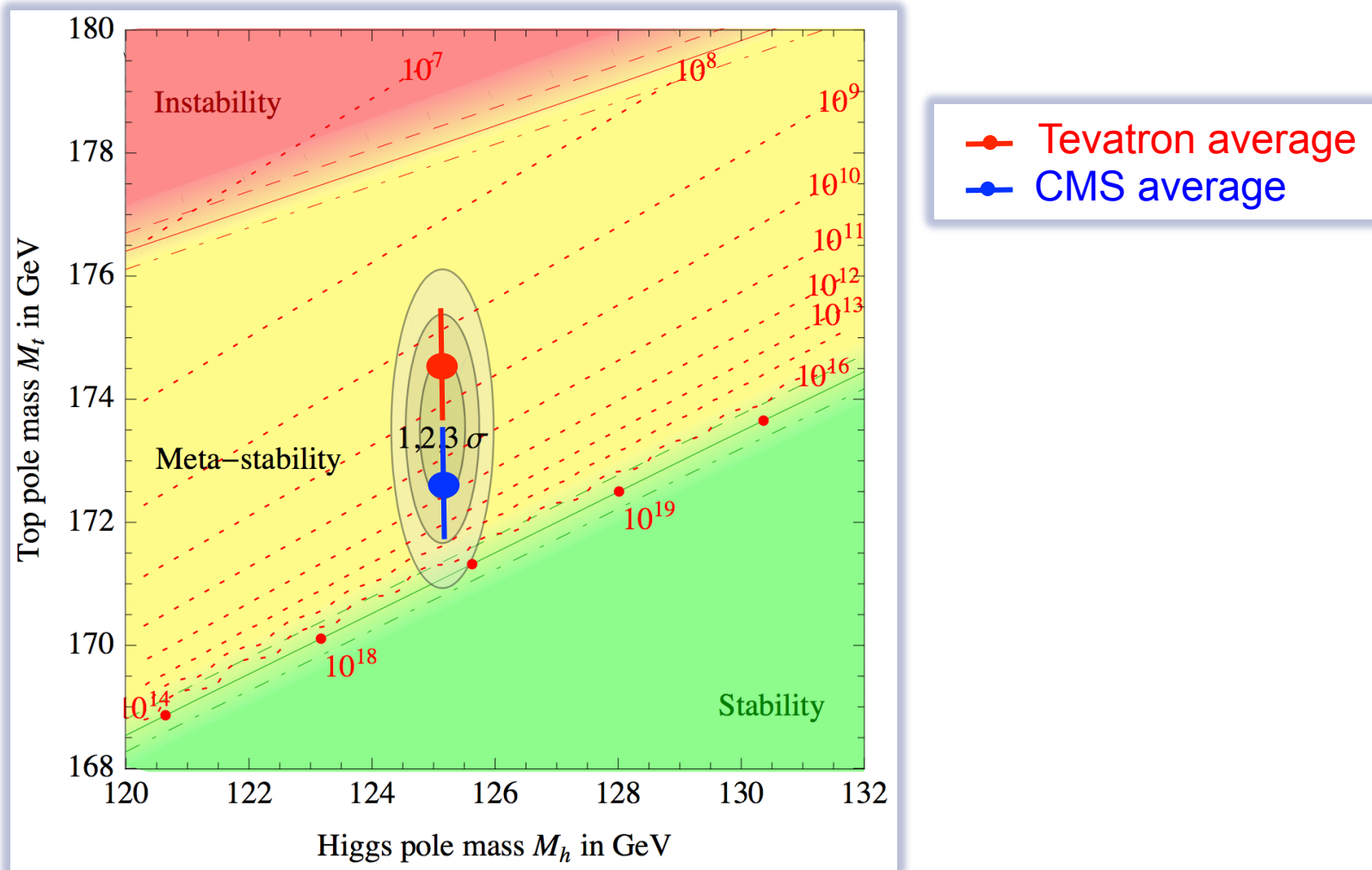
- I have shown some of:
 - the world's best results
 - the innovative approaches
- Summary of best results →
- How does it all fit together?
 - Tevatron average higher than world average (driven by DØ)
 - CMS average lower than world average
 - → interpretation?
- Unfortunately,
 - no time to talk about indirect measurements in a well-defined scheme





EW precision data and the Higgs mass tend to have a slight preference for recent Tevatron m_t results, CMS a bit further away

Summary: stability of the EW vacuum



Recent Tevatron m_t results indicate a shorter lifetime of the Universe
 → Potential contributions from new particles to running group equation?